

Accepted Manuscript

Design and synthesis of benzodiazepine analogs as isoform-selective human lysine deacetylase inhibitors

D. Rajasekhar Reddy, Flavio Ballante, Nancy J. Zhou, Garland R. Marshall



PII: S0223-5234(16)31038-8

DOI: [10.1016/j.ejmech.2016.12.032](https://doi.org/10.1016/j.ejmech.2016.12.032)

Reference: EJMECH 9123

To appear in: *European Journal of Medicinal Chemistry*

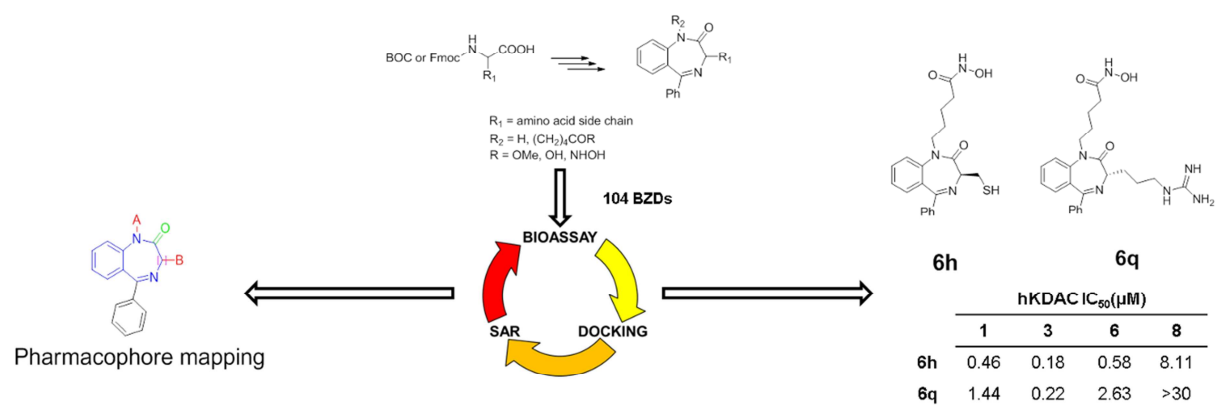
Received Date: 8 November 2016

Revised Date: 30 November 2016

Accepted Date: 16 December 2016

Please cite this article as: D.R. Reddy, F. Ballante, N.J. Zhou, G.R. Marshall, Design and synthesis of benzodiazepine analogs as isoform-selective human lysine deacetylase inhibitors, *European Journal of Medicinal Chemistry* (2017), doi: 10.1016/j.ejmech.2016.12.032.

This is a PDF file of an unedited manuscript that has been accepted for publication. As a service to our customers we are providing this early version of the manuscript. The manuscript will undergo copyediting, typesetting, and review of the resulting proof before it is published in its final form. Please note that during the production process errors may be discovered which could affect the content, and all legal disclaimers that apply to the journal pertain.



Design and Synthesis of Benzodiazepine Analogs as Isoform-Selective Human Lysine Deacetylase Inhibitors

D. Rajasekhar Reddy, Flavio Ballante, Nancy J. Zhou, and Garland R. Marshall*

Department of Biochemistry and Molecular Biophysics, Washington University School of Medicine, St. Louis, MO 63110

*Corresponding author E-mail: garlandm@gmail.com (Garland R. Marshall)

ABSTRACT

A comprehensive investigation was performed to identify new benzodiazepine (BZD) derivatives as potent and selective human lysine deacetylase inhibitors (hKDACis). A total of 108 BZD compounds were designed, synthesized and from that 104 compounds were biologically evaluated against human lysine deacetylases (hKDACs) 1, 3 and 8 (class I) and 6 (class IIb). The most active compounds showed mid-nanomolar potencies against hKDACs 1, 3 and 6 and micromolar activity against hKDAC8, while a promising compound (**6q**) showed selectivity towards hKDAC3 among the different enzyme isoforms. An hKDAC6 homology model, refined by molecular dynamics simulation was generated, and molecular docking studies performed to rationalize the dominant ligand-residue interactions as well as to define structure-activity-relationships. Experimental results confirmed the usefulness of the benzodiazepine moiety as capping group when pursuing hKDAC isoform-selectivity inhibition, suggesting its continued use when designing new hKDACis.

KEYWORDS

Epigenetics; Histone Deacetylase (HDAC); Lysine Deacetylase (KDAC); Benzodiazepine (BZD); Structure-based drug design (SBDD)

INTRODUCTION

Being an epigenetic target, lysine deacetylases (KDACs) generally referred to as histone deacetylases (HDACs), are a family of enzymes that are responsible for deacetylation of lysine residues in both histone and non-histone substrates [1], emerged as an important target in the development of potential therapeutic agents [2-6]. These enzymes are involved in a wide variety biological processes, including cell differentiation, angiogenesis, and apoptosis [3, 7, 8]. The 18 isoforms of KDAC are classified into four distinct groups: class I (KDACs 1, 2, 3, and 8), class II (class IIa (KDACs 4, 5, 7, and 9), class IIb (KDACs 6 and 10)), class III (sirtuins) and class IV (KDAC11) based on their size, number of catalytically active sites, subcellular locations, and sequence homology with respect to their yeast counterparts [9-12]. Except for class III KDACs (sirtuins) that are NAD^+ -dependent proteins, the other enzymes are all zinc dependent [9, 13, 14].

Numerous structurally diverse KDACs inhibitors (KDACis) against Zn^{2+} -dependent KDACs have been explored [15, 16], and some of them FDA approved while others are at various stages of clinical evaluation [17, 18]. Romidepsin (FK-228) [19, 20], vorinostat (SAHA) [21], belinostat (PXD101) [22], and panobinostat (LBH589) [23, 24], (**Figure 1**) have been approved by the U.S. Food and Drug Administration (FDA) for the treatment of cutaneous T-cell lymphoma (CTCL), peripheral T-cell lymphoma (PTCL), and multiple myeloma, respectively. Chidamide, a KDACi developed in China, has been recently approved by the China Food and

Drug Administration for the treatment of PTCL [25]. However, most KDACis are class I selective (FK-228, PXD101) or pan-KDAC inhibitors (SAHA, LBH589). These nonselective or partially selective KDAC inhibitors usually lead to undesirable biological side effects, such as fatigue, nausea, and cardiotoxicity [26-30]. To avoid the side effects, an increasing number of investigations are focusing on the development of isotype-selective KDAC inhibitors [14, 17]. In continuation of these efforts, benzodiazepines (BZDs) have also been used as cap groups to discover isoform-selective KDAC inhibitors (**Figure 2**) [31, 32]. During the course of our investigation, an article appeared that also utilized BZD as a cap group (**Figure 2**) [33, 34].

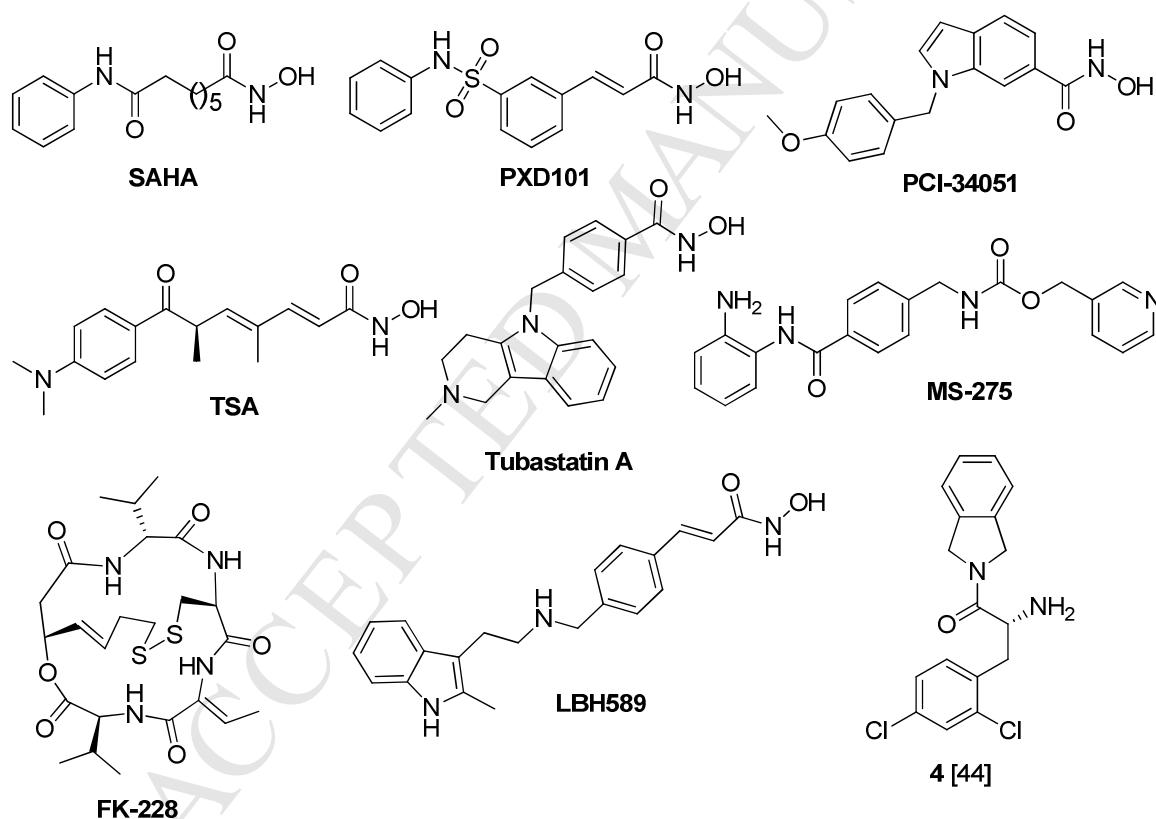


Figure 1. Examples of potent KDAC inhibitors.

Herein, we report the design of novel C3-substituted benzodiazepines with an amino acid side chain as cap group and at N1 linear alkyl chain bearing different functions as the Zn^{2+} -chelating group (**Figure 2**) targeting human lysine deacetylase (hKDAC) isoforms based on analysis of structure-activity relationships (SARs); a library of BZD analogs has been synthesized. The lead compounds from this library exhibit potent class I KDAC selectivity.

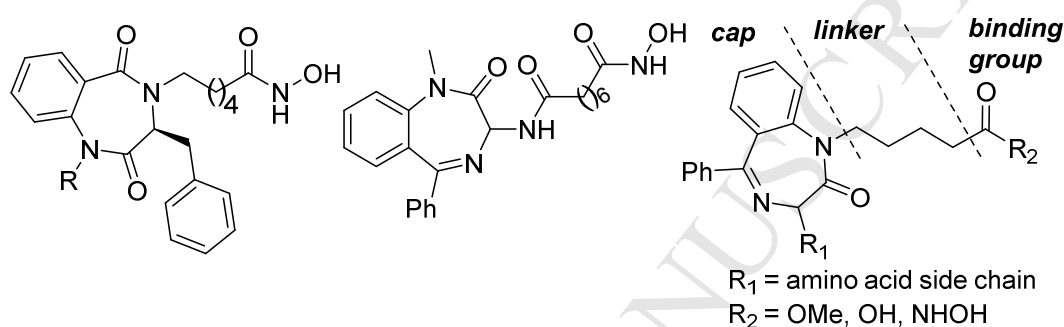
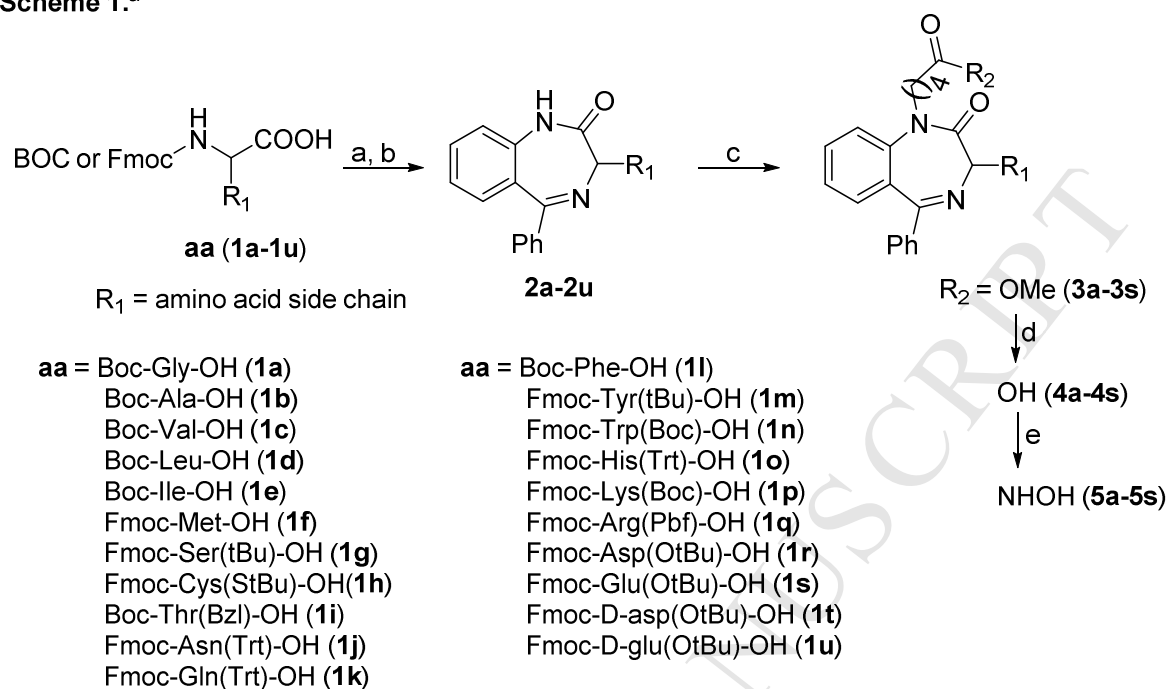


Figure 2. KDAC inhibitors with BZD scaffold as cap group.

RESULTS

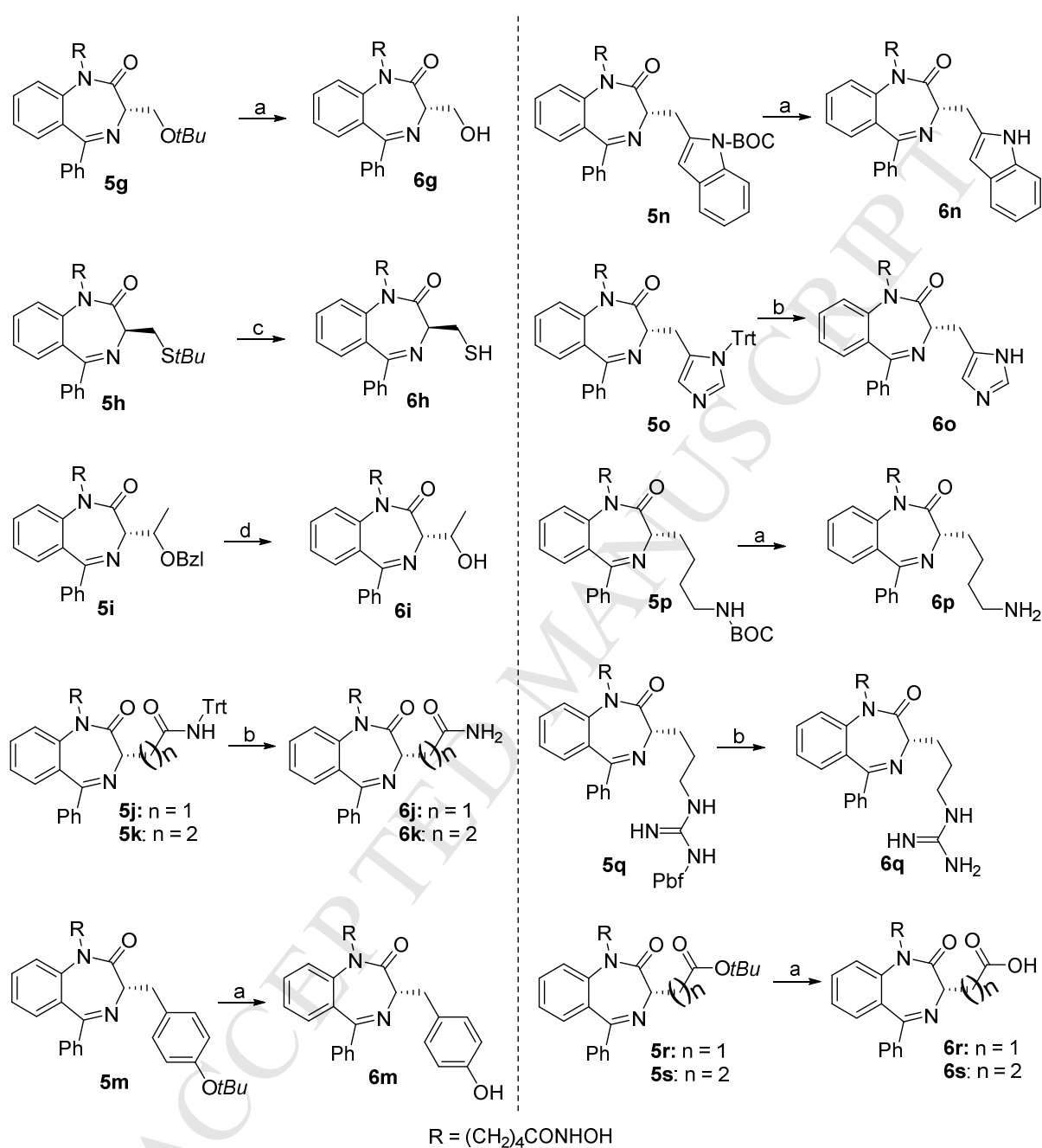
Chemistry

C3-substituted BZDs (**2a-2u**) were synthesized from readily available 2-aminobenzophenone in a three-step process, often without the need for purification until the cyclization step. N1-Substituted BZD analogs (**3a-3s**) were synthesized by treating BZDs (**2a-2s**) with sodium hydride and alkylation with methyl-5-bromovalerate in DMF at room temperature. BZD acids (**4a-4s**) were obtained by the hydrolysis of BZD-methyl esters (**3a-3s**) with 1M KOH aqueous solution in MeOH or by using LiOH in MeOH/ H_2O (9:1). BZD hydroxamic acids (**5a-5s**) were generated with a mixed anhydride approach with ethyl chloroformate (ECF) and reacting with $\text{NH}_2\text{OH}\cdot\text{HCl}$ (**Scheme 1**).

Scheme 1.^a

^aReagents and Conditions: a. (i) *N*-methylmorpholine, THF, -20 °C, ethyl chloroformate, 15 min., (ii) 2-aminobenzophenone; b. (i) TFA, DCM, 0 °C-rt (for BOC), or 20% piperidine in DCM, rt (for Fmoc), (ii) $\text{CH}_3\text{COONH}_4$, AcOH, rt; c. methyl-5-bromovalerate, NaH, DMF, rt, 12h; d. 1M KOH aq., MeOH, rt, 12h, (for **4r**, **4s**: LiOH, MeOH : H_2O (9:1), rt, 12h); e. (i) *N*-methylmorpholine, THF, -20 °C, ethyl chloroformate, 15 min., (ii) $\text{NH}_2\text{OH}\cdot\text{HCl}$, H_2O , rt, 1-12h.

Finally, the BZD hydroxamates with free side chain were obtained by cleaving the protecting groups. BZD hydroxamates **6g**, **6m**, **6r**, **6s**, **6n**, and **6p** were obtained by cleaving the protecting groups on **5g**, **5m**, **5r**, **5s**, **5n**, and **5p** compounds side chain with TFA. Side chain protecting groups cleavage with TFA/ TIS on compounds **5j**, **5k**, **5o**, and **5q** provided hydroxamate BZDs **6j**, **6k**, **6o**, and **6q**. Compound **6h** was obtained from **5h** by employing the trifluoromethanesulfonic acid and debenzoylation of **5i** with excess of $\text{BF}_3\cdot\text{OEt}_2$ and EtSH afforded **6i** (Scheme 2).

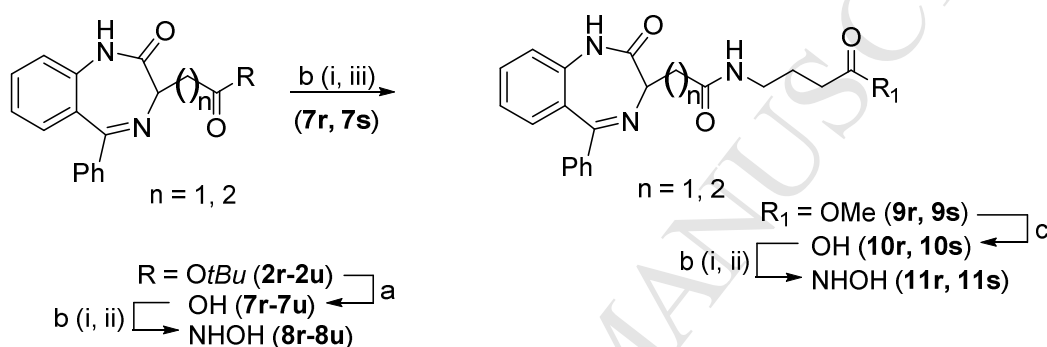
Scheme 2.^a

^aReagents and Conditions: a. TFA, rt, 4h; b. TFA/ TIS, rt, 4h; c. CF₃SO₃H, rt, 4h; d. BF₃·OEt₂, EtSH, rt, 6h.

BZD compounds (**8r-8u**) were synthesized by mixed anhydride formation from their acids (**7r-7u**), which were obtained by *tert* butyl deprotection of **2r-2u** compounds with TFA. BZD hydroxamates (**11r, 11s**) were obtained from BZD acids **7r, 7s** by mixed anhydride approach and

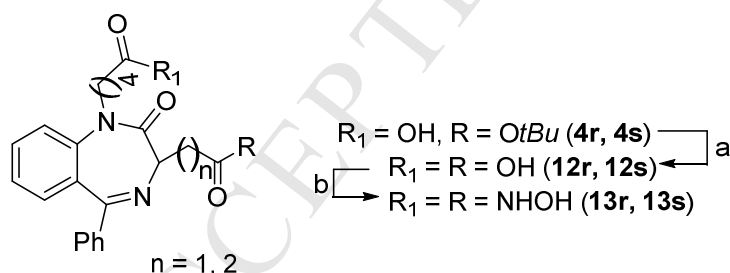
reacting with methyl-4-aminobutanoate HCl salt [35]. The resulted esters **9r**, **9s** on hydrolysis provided acids **10r**, **10s**. These acids are converted to hydroxamic acids **11r**, **11s** by reacting with hydroxylamine HCl salt (**Scheme 3**). BZDs **13r**, **13s** were synthesized by mixed anhydride formation from their acids (**12r**, **12s**), which were obtained by *tert* butyl deprotection of compounds **4r**, **4s** with TFA (**Scheme 4**).

Scheme 3.^a



^aReagents and Conditions: a. TFA, rt, 4h; b. (i) *N*-methylmorpholine, THF, -20 °C, ethyl chloroformate, (ii) $\text{NH}_2\text{OH}\cdot\text{HCl}$, H_2O , rt, 12h; (iii) $\text{NH}_2(\text{CH}_2)_3\text{COOMe}\cdot\text{HCl}$, H_2O , rt, 12h; c. 1M KOH aq., MeOH, rt, 12h.

Scheme 4.^a



^aReagents and Conditions: a. TFA, rt, 4h; b. (i) *N*-methylmorpholine, THF, -20 °C, ethyl chloroformate, (ii) $\text{NH}_2\text{OH}\cdot\text{HCl}$, H_2O , rt, 12h.

Bioactivity Against Isolated hKDAC Isoforms

All the synthesized BZD derivatives were assayed (for details, see the Experimental Section) for their inhibitory activity against recombinant hKDACs 1, 3 and 8 (Class I KDACs) and hKDAC 6

(Class II KDACs). *In vitro* assays were performed using the Caliper EZ Reader II system (Perkin-Elmer Caliper Life Sciences, USA). The candidates were firstly tested in duplicate at 30 μ M (see Supplementary material **Tables S3-S4** for all the BZDs inhibitor % values over the 4 considered hKDACs). Those compounds showing an inhibitory activity $\geq 50\%$ at 30 μ M were then assayed using two replicates in a 10-point dose curve with 3-fold serial dilution starting from 30 μ M, for which IC_{50} values as well as dose-response curves were then derived (**Tables 1 and 2** and Supplementary material **Table S5** for dose-response curves). As positive controls ten well-known hKDACis were used (**Table 3**, Supplementary material **Table S6** for dose-response curves).

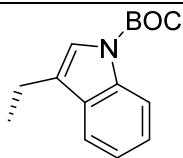
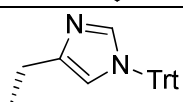
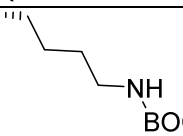
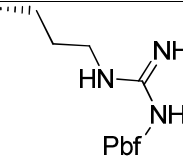
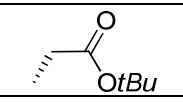
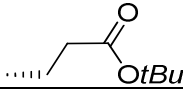
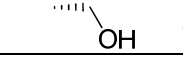
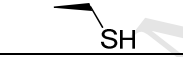
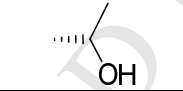
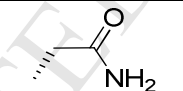
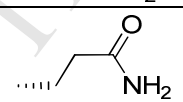
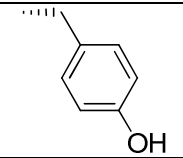
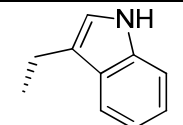
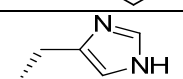
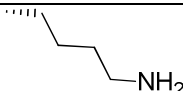
Table 1. C3-substituted BZD analogs hKDAC IC_{50} (μ M) values.

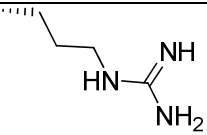
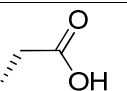
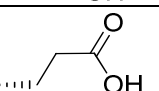
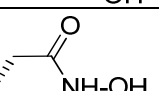
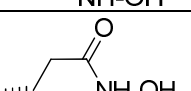
Entry ^a	ID	R ₁	Biological response ^b			
			IC_{50} (μ M) ^c			
			hKDAC isoform			
			1	3	6	8
1	8s		16.92	>30	>30	>30
2	11r		17.38	3.21	1.76	>30
3	11s		22.87	5.17	7.16	>30

^aOnly compounds showing at least one detectable IC_{50} are reported (see Supplementary material **Table S3** for the complete list). ^bCompounds were tested in a 10-point dose with 3-fold serial dilution starting from 30 μ M. ^c IC_{50} values and dose-response curves were derived for compounds with inhibition $\geq 50\%$ at 30 μ M. See Supplementary material **Tables S3** and **S5** for all inhibition data and dose-response curves.

Table 2. N1, C3-Substituted BZD analogs hKDAC IC₅₀ (μM) values.

Entry ^a	ID	R ₁	Biological response ^b IC ₅₀ (μM) ^c hKDAC isoform			
			1	3	6	8
1	5a	H	3.84	0.66	1.89	6.72
2	5b	Me	12.67	1.80	2.95	24.75
3	5c		5.27	0.60	1.35	19.83
4	5d		5.90	0.57	2.33	>30
5	5e		10.96	1.03	3.75	>30
6	5f		6.43	0.43	1.70	20.28
7	5g		9.00	1.21	5.05	>30
8	5h		7.99	0.75	5.37	>30
9	5i		4.55	0.91	2.05	29.54
10	5j		>30	4.31	6.27	>30
11	5k		9.24	0.83	0.99	23.48
12	5l		8.51	0.49	1.98	12.67
13	5m		6.18	0.85	2.87	3.30

14	5n		>30	5.21	6.92	8.39
15	5o		>30	2.55	4.74	>30
16	5p		4.63	0.59	3.06	21.79
17	5q		>30	4.29	16.17	>30
18	5r		15.7	4.15	6.43	22.39
19	5s		4.57	1.03	2.35	26.07
20	6g		>30	4.94	6.35	>30
21	6h		0.46	0.18	0.58	8.11
22	6i		11.23	1.80	11.58	>30
23	6j		22.53	3.10	5.38	>30
24	6k		13.95	1.94	1.29	>30
25	6m		>30	5.29	8.46	>30
26	6n		16.84	1.01	1.95	>30
27	6o		13.88	1.32	4.98	>30
28	6p		6.54	0.95	12.12	>30

29	6q		1.44	0.22	2.63	>30
30	6r		>30	12.60	19.84	>30
31	6s		>30	8.71	16.00	>30
32	13r		9.99	10.39	>30	>30
33	13s		14.97	2.57	1.74	8.52

^aOnly compounds showing at least one detectable IC₅₀ are reported (see Supplementary material Table S3 for the complete list). ^bCompounds were tested in a 10-point dose with 3-fold serial dilution starting from 30 μM. ^cIC₅₀ values and dose-response curves were derived for compounds with inhibition ≥50% at 30 μM. See Supplementary material **Tables S4** and **S5** for all inhibition data and dose-response curves.

Table 3. Standard compounds (positive controls) hKDAC IC₅₀ (μM) values.

Entry	ID	Biological response ^a IC ₅₀ (μM) ^b KDAC isoform			
		1	3	6	8
1	Entinostat (MS-275) [36]	1.48 [35]	0.79 [35]	>30 [35]	>30 [35]
2	Largazole^c [37]	2.33 [35]	1.36 [35]	9.29 [35]	>30 [35]
3	Panobinostat (LBH589) [23, 24]	0.02	0.06	0.13	1.78
4	PCI-34051 [38]	14.41 [35]	>30 [35]	4.57 [35]	0.49 [35]
5	SD-L-256 [39]	3.48 [35]	0.47 [35]	1.61 [35]	>30 [35]
6	Trichostatin A (TSA) [40]	0.015 [35]	0.020 [35]	0.038 [35]	4.55 [35]
7	Tubastatin A [41]	2.87 [35]	0.77 [35]	0.014 [35]	2.34 [35]
8	T247 [42]	1.11 [35]	3.94 [35]	>30 [35]	>30 [35]
9	Vorinostat (SAHA) [43]	0.0070 [35]	0.0014 [35]	0.0014 [35]	0.50 [35]
10	4 [44]	27.37	20	>30	1.09

^aCompounds were tested in a 10-point dose with 3-fold serial dilution starting from 30 μM.

^bIC₅₀ values and dose-response curves were derived for compounds with inhibition ≥ 50% at 30 μM. ^cThe thioester form of largazole was assayed as previously reported [35].

See Supplementary material **Table S6** for dose-response curves.

Inhibitor Potency. Among the BZD compounds, the highest inhibitor activities were generally detected towards the hKDAC3 isoform (**Tables 1 and 2**): **6h** (a N1, C3-substituted BZD) showed the highest potency against hKDAC3 ($IC_{50} = 180$ nM), with a mid-nanomolar activity against hKDACs 1 and 6 ($IC_{50} = 460$ nM and 580 nM, respectively) and a low micromolar inhibition against hKDAC8 ($IC_{50} = 8.11$ μ M). Compound **6h** was the only BZD endowed with an IC_{50} value lower than 1 μ M against hKDAC1 and hKDAC6 (as reported above), together with **5k** (a N1, C3-substituted BZD having an $IC_{50} = 990$ nM vs hKDAC6). Similarly as **6h**, compound **6q** (a N1, C3-substituted BZD) showed an IC_{50} value of 220 nM against hKDAC3, but a lower activity (thus higher selectivity) when considering the other 3 isoforms (IC_{50} values of 1.44 μ M, 2.63 μ M and >30 μ M against hKDAC1, 6 and 8, respectively). Other 11 BZD compounds (**5f**, **5l**, **5d**, **5p**, **5c**, **5a**, **5h**, **5k**, **5m**, **5i** and **6p**; all N1, C3-substituted BZDs) were detected to be most active against the hKDAC3 isoform showing an $IC_{50} \sim 1\mu$ M. No BZD derivatives showed interesting inhibitor activity against hKDAC8: **5m** ($IC_{50} = 3.3$ μ M) was detected as the most active.

Isoform Selectivity. By comparing the 104-benzodiazepine derivatives with their relative isoform-related activities (**Tables 1-2** and Supplementary material **Tables S3-S4**), it was possible to rationalize a series of features required for inhibitory potency and isoform selectivity. *hKDAC1.* 28 BZDs showed an inhibitory percentage value greater than 50% at 30 μ M (with a range of IC_{50} values comprised between 460 nM and 22.87 μ M; only compound **6h** showed an $IC_{50} < 1\mu$ M). Among them, only three C3-substituted BZDs (**8s**, **11r**, **11s**) were detected, but showing lower inhibitory activities (IC_{50} values of 16.92 μ M, 17.38 μ M and 22.87 μ M, respectively). All of the derivatives with an $IC_{50} < 30\mu$ M were hydroxamic acids. Conversely, those compounds without inhibitory activity had no hydroxamic moiety as a zinc-binding group,

confirming the effectiveness of this moiety for ligand-protein recognition: for example, compounds **5a** and **4a** (both are N1, C3-substituted, with a hydrogen in C3, and 4 carbon atoms as linker in N1) differ only by the presence of the hydroxamic moiety (characterizing **5a**), but show a completely different hKDAC1 inhibition activity ($IC_{50} = 3.84 \mu M$ and $>30 \mu M$, respectively).

About the C3-substituted derivatives, the C3 configuration affected the biological response; the L-derivatives were more active than those compounds with a D-configuration. For example, compound **8s** (a C3-substituted BZD), having a (*L*)-C3, has a higher activity ($IC_{50} = 16.92 \mu M$) than its enantiomer (compound **8u**, $IC_{50} >30 \mu M$), thus suggesting a primary role of the C3 configuration in BZD-hKDAC1 recognition.

hKDAC3. Compared to hKDAC1, a higher number of tested compounds (a total of 35) showed an inhibition percentage greater than 50% at $30 \mu M$ (IC_{50} values between 180 nM and $12.6 \mu M$). Of those, thirteen showed an $IC_{50} \sim 1 \mu M$. Noteworthy, the highest inhibition potencies were obtained against this enzyme isoform (e.g. compounds **6h** and **6q** as reported above). Among those derivatives showing an $IC_{50} <30 \mu M$, only two are C3-substituted (**11r** and **11s**, IC_{50} values of $3.21 \mu M$ and $5.17 \mu M$, respectively); interestingly, even those with a 6- or 7-atom linkers showed higher activities compared to hKDAC1 (IC_{50} values equal to $17.38 \mu M$ and $22.87 \mu M$, respectively). This suggests that hKDAC3 accepts ligands characterized by a longer linker. Similar to hKDAC1, all of the derivatives with $IC_{50} <30 \mu M$ are hydroxamic acids, but the D/L configuration at C3 (when considering C3-substituted derivatives), gave an opposite effect on hKDAC3 inhibition compared to the hKDAC1 case: for example, compound **8u** (D-derivative) showed a higher inhibition percentage (29.45% at $30 \mu M$) with respect to its L-enantiomer (4.57% at $30 \mu M$, see Supplementary material **Table S3**).

hKDAC6. 34 BZD compounds showed an inhibition percentage greater than 50% at 30 μ M (with a range of IC_{50} values comprised between 580 nM and 19.84 μ M); only two from this series (**6h** and **5k**), had an $IC_{50} \leq 1 \mu$ M (580 nM and 990 nM respectively). As for *hKDAC1* and 3, among the most active derivatives (those with an $IC_{50} \leq 30 \mu$ M), only two (**11r** and **11s**, IC_{50} values equal to 1.76 μ M and 7.16 μ M, respectively) are C3-substituted, while all are hydroxamic acids. Thus, similar to *hKDAC3*, ligands characterized by a longer linker are well accepted by *hKDAC1*. The effect of the D/L-configuration at C3 (for C3-substituted derivatives) is similar to the case of *hKDAC1*; the L-configuration increased the inhibition potency (i.e. **8s**, an L-derivative showing an inhibition of 36.51% at 30 μ M was more active than its enantiomer **8u** which has approximatively half the potency, 19.02% at 30 μ M, see Supplementary material **Table S3**).

hKDAC8. Compared to the other isoforms, *hKDAC8* was generally less inhibited by the tested compounds. In fact, only 14 BZDs resulted with an inhibition percentage value greater than 50% at 30 μ M (showing a range of IC_{50} values comprised between 3.3 μ M and 29.5 μ M), and none of these with an $IC_{50} \leq 1 \mu$ M. Similarly to the results for the other isoforms, the most active compounds (with an $IC_{50} \leq 30 \mu$ M) were hydroxamic acids, but (conversely from the other targeted enzymes) none of them were C3-substituted derivatives. The first four most active compounds are **5m**, **5a**, **6h** and **5n** ($IC_{50} = 3.30 \mu$ M, 6.72 μ M, 8.11 μ M and 8.39 μ M, respectively), characterized by Tyr(tBu), Gly, Cys and Trp(Boc) amino acid side chains suggest that aromatic rings with terminal aliphatic chains (as in **5m** and **5n**) or short aliphatic/polar moieties (as in **5a** and **6h**) are preferred (e.g. compare **5m** with **5l**; **5n** with **6n**). To the contrary, the low activity of **6q** and **6p** (characterized by an Arg and Lys) indicates the negative impact of a positively charged group on *hKDAC8* inhibition.

Isoform Selectivity. Beside the inhibitory potency, isoform selectivity is an important issue during the discovery of new KDACis. Given the number of enzyme isoforms herein, we propose to summarize the selectivity of an inhibitor using a global isoform-selectivity index (GISIndex) for each specific hKDAC isoform. To obtain the GISIndex, all the partial selectivity indexes towards each investigated isoform were derived (SIs, Supplementary material **Table S7**), and the average computed. When considering hKDACs 1, 3, 6 and 8, for each enzyme isoform, three partial selectivity indexes (SIs) can be derived. As an example, when considering hKDAC1, three SIs can be computed: from hKDAC3 (denoted as 1/3), hKDAC6 (denoted as 1/6), and hKDAC8 (denoted as 1/8); then the hKDAC1 GISIndex is derived by averaging the three partial SIs (Supplementary material **Table S7**). As a result, a selective KDACi will show a higher GISIndex coefficient only towards one hKDAC isoform. **Table 4** reports the positive GISIndexes characterizing the tested compounds (BZDs and standards) while those with a GISIndex equal to zero are omitted (see Supplementary material **Table S7** for the complete table of results). Tubastatin A was the most selective compound, showing one relevant GISIndex (142.38) towards hKDAC6, while compounds characterized by at least two similar GISIndexes among the enzyme isoforms, were not as selective (e.g. TSA and SAHA, as expected since they are characterized as pan-inhibitors). Among the BZD derivatives, compound **6q** was the most selective with a detectable preference for hKDAC3 (GISIndex = 51.62, and negligible values from the other isoforms), followed by a series of BZDs: **5d**, **5f**, **5h**, **6p**, **6h**, **5p**, **5l** and **6n** with a hKDAC3 GISIndex greater than 15 while negligible for other isoforms (**Table 4**). All of the 9 compounds composing the above series, are N1, C3-substituted BZD analogs and hydroxamic acids; moreover, even if characterized by different amino acid chains, their activity range against

hKDAC3 varies by only a factor of 5.61 (being **6h** the most active and **6n** the least active, showing an IC_{50} = 180 nM and 1.01 μ M, respectively).

Table 4. hKDACs 1, 3, 6 and 8 global isoform selectivity indexes. The tested compounds have been ranked for each isoform according to the relative global isoform selectivity index value. Standard compounds are reported as italic characters.

hKDAC1		hKDAC3		hKDAC6		hKDAC8	
GIS Index ^a	ID	GIS Index ^a	ID	GIS Index ^a	ID	GIS Index ^a	ID
102.40	<i>TSA</i>	120.71	<i>SAHA</i>	142.38	<i>Tubastatin A</i>	33.32	<i>PCI-34051</i>
32.83	<i>LBH589</i>	75.83	<i>TSA</i>	120.71	<i>SAHA</i>	23.66	<i>4</i>
23.81	<i>SAHA</i>	51.62	<i>6q</i>	39.91	<i>TSA</i>	1.19	<i>5n</i>
19.20	<i>T247</i>	25.32	<i>MS-275</i>	11.86	<i>6k</i>	0.62	<i>5m</i>
13.51	<i>MS-275</i>	24.89	<i>SD-L-256</i>	11.02	<i>5k</i>	0.59	<i>13s</i>
7.55	<i>6q</i>	22.36	<i>5d</i>	9.58	<i>11r</i>	0.41	<i>Tubastatin A</i>
6.30	<i>6h</i>	22.02	<i>5f</i>	8.01	<i>6n</i>		
5.62	<i>Largazole</i>	19.27	<i>5h</i>	6.93	<i>SD-L-256</i>		
2.87	<i>SD-L-256</i>	17.07	<i>6p</i>	6.20	<i>5c</i>		
2.35	<i>13r</i>	16.94	<i>6h</i>	5.54	<i>5i</i>		
2.16	<i>5i</i>	16.66	<i>5p</i>	5.24	<i>5f</i>		
2.15	<i>6p</i>	15.76	<i>5l</i>	5.14	<i>5d</i>		
1.90	<i>5s</i>	15.46	<i>6n</i>	4.99	<i>13s</i>		
1.77	<i>8s</i>	14.69	<i>5c</i>	4.66	<i>6h</i>		
1.69	<i>5d</i>	14.47	<i>5e</i>	4.56	<i>LBH589</i>		
1.57	<i>5p</i>	13.24	<i>5i</i>	4.35	<i>5s</i>		
1.25	<i>5c</i>	13.14	<i>5k</i>	4.23	<i>5b</i>		
1.25	<i>5h</i>	12.34	<i>6o</i>	4.22	<i>5o</i>		
1.23	<i>6i</i>	12.13	<i>5g</i>	3.80	<i>6q</i>		
1.11	<i>5g</i>	10.68	<i>5s</i>	3.64	<i>5e</i>		
1.05	<i>5f</i>	10.61	<i>LBH589</i>	3.57	<i>5l</i>		
0.91	<i>5e</i>	9.78	<i>6i</i>	3.25	<i>6j</i>		
0.85	<i>5k</i>	9.63	<i>Largazole</i>	3.24	<i>PCI-34051</i>		
0.72	<i>6o</i>	7.84	<i>5o</i>	3.19	<i>5j</i>		
0.72	<i>6k</i>	7.55	<i>6k</i>	3.15	<i>6g</i>		
0.69	<i>PCI-34051</i>	6.93	<i>5b</i>	2.94	<i>6o</i>		
0.65	<i>5b</i>	6.29	<i>5a</i>	2.88	<i>5p</i>		
0.59	<i>6n</i>	5.92	<i>5q</i>	2.57	<i>5g</i>		
0.58	<i>5a</i>	5.65	<i>6j</i>	2.46	<i>11s</i>		
0.58	<i>11r</i>	5.08	<i>T247</i>	2.36	<i>6m</i>		
0.50	<i>5l</i>	4.92	<i>11r</i>	2.36	<i>5h</i>		
0.48	<i>5r</i>	4.84	<i>5m</i>	1.97	<i>5r</i>		
0.44	<i>6j</i>	4.64	<i>5j</i>	1.86	<i>5a</i>		
0.44	<i>11s</i>	4.05	<i>6g</i>	1.85	<i>5n</i>		
0.37	<i>4</i>	3.78	<i>6m</i>	1.25	<i>6s</i>		
		3.41	<i>11s</i>	1.24	<i>5q</i>		
		3.06	<i>5r</i>	1.10	<i>5m</i>		
		3.05	<i>13s</i>	1.08	<i>Largazole</i>		
		2.30	<i>6s</i>	1.01	<i>6r</i>		
		2.26	<i>Tubastatin A</i>	0.86	<i>6i</i>		
		1.92	<i>13r</i>	0.83	<i>6p</i>		
		1.92	<i>5n</i>				
		1.59	<i>6r</i>				

^aGlobal Isoform Selectivity Index (GISIndex): is the average value of all the partial selectivity indexes when considering a certain hKDAC isoform (see Supplementary material **Table S7**).

Among these 9 compounds, even with a polar or charged R_1 group (cysteine or arginine) had the highest hKDAC3 inhibition potency (as **6h** and **6q** showing $IC_{50} = 180$ nM and 220 nM respectively), the presence of a hydrophobic, or aromatic amino acid still guaranteed a decent activity (e.g. **5l** or **6n** which are characterized by a phenylalanine or tryptophan, showed $IC_{50} = 490$ nM and 1.01 μ M respectively), suggesting a high degree of active-site flexibility by hKDAC3. Conversely, the discriminatory effect of the different R_1 groups was dramatically higher when considering hKDAC1 and hKDAC6 among this series of 9 compounds. In fact, the hKDAC1 inhibitor potencies drastically decrease when a polar amino acid (like a cysteine or arginine characterizing **6h** and **6q** respectively) was replaced with a hydrophobic one (a leucine as in **5d**), even more if an aromatic ring was present (phenylalanine or tryptophan in **5l** and **6n** respectively). Interestingly, **6p** (characterized by a lysine at R_1) was a weaker hKDAC1 inhibitor compared to **6q** (an arginine derivative), thus suggesting the positive effect of having a guanidinium group (as in **6q** respect that one in **6p**). Conversely, hKDAC6 inhibition was not much affected with bulky groups present at R_1 (tryptophan or phenylalanine in **6n** and **5l** respectively). Lastly, the weak hKDAC8 inhibition from this series of 9 compounds suggests a lack of specific chemical interactions for enzyme inhibition; a decrease of inhibition effect is observed when considering a short and polar amino acid group (cysteine in **6h**, $IC_{50} = 8.11$ μ M) was replaced by a longer and charged/polar one (i.e. **6q** and **6p**, characterized by an arginine or lysine, respectively with both showing an $IC_{50} > 30$ μ M).

Two compounds, **6k** and **11r**, were more selective towards hKDAC6 (**Table 4**), while **5k** having similar GISIndexes values for hKDAC3 and 6 (13.14 and 11.02, respectively) cannot be considered as selective. Interestingly, **6k**, **11r** and **5k** all featured an amide group characterizing the cap portion, suggesting a potential role of this moiety when targeting hKDAC6 selectivity. To further clarify the discriminatory BZDs-hKDACs interaction as well as those necessary for inhibition potency, molecular modeling studies were performed.

Molecular Modeling

To rationalize the biochemical results and the isoform selectivity, a comparative structure analysis was performed among the 4 selected hKDAC isoforms also used as targets for molecular docking of the synthesized 104 BZD derivatives (**Tables 1** and **2**, Supplementary material **Tables S3-S4**) as well as standard compounds (positive controls, **Table 3**). Crystal structures of hKDAC1, hKDAC3, and hKDAC8 (PDB codes 4BKX, 4A69, 3RQD, respectively) were prepared as previously reported [45], while a hKDAC6 homology model was derived and refined with molecular dynamics simulation.

hKDAC6 model generation

The homology model (a hKDAC6-SAHA complex) was generated and subsequently submitted to MD simulation for 95 ns to study the protein's structural flexibility and to obtain a refined model to be used during docking studies (see Molecular Modeling section in Supplementary material). SAHA was included in the active site during model generation, due to its high inhibitory activity against the hKDAC6 ($IC_{50} = 1.4$ nM, **Table 3**) and to prevent collapse of the active site, thus providing a reasonable model structure to be used for future docking. Multiple crystallographic structures of human and zebrafish KDAC6 catalytic domains (hCD1 and hCD2,

and zCD1 and zCD2, respectively), released [46, 47] when our study was completed, provided a template for validation of our hKDAC6 homology model (see Supplementary material **Figure S3**). By superimposing our KDAC6 homology model with the relative X-ray protein structure (PDB code: 5EDU) [46] an RMSD of 1.05Å was detected, suggesting a general good approximation of the predicted model's backbone. As expected, major conformational differences were detected for residues characterizing an important loop for molecular recognition of ligands endowed with high conformational variability (see Supplementary material **Figure S3C**), as a reasonable result of the different bound ligand (SAHA in the homology model and TSA in the X-ray complex), and experimentally supported by the different bioactivity of the two hydroxamic acid derivatives (27-fold IC₅₀ difference, see **Table 3**).

hKDACs 1, 3, 6 and 8 structural comparison.

By superimposing the four hKDAC isoforms (1, 3, 6 and 8, **Figure 3A**), one can highlight sequence conservation percentages, i.e., for those amino acid portions (close to the active site) characterized by the highest variability and involved in enzyme selectivity (**Figure 3B**). Five sequences (1 to 5, **Figure 3C**; see Supplementary material **Figure S4**) were selected and compared (**Figure 4**).

Sequence 1. The characterizing loop (**Figure 4**, Supplementary material **Figure S4**) has a similar residue sequence when hKDAC1 and 3 are considered (Gln26-Gly27-His28-Pro29-Met30-Lys31 versus Ala20-Gly21-His22-Pro23-Met24-Lys25, respectively), while more differences were detected in hKDAC6 (Ser498-His499-His500-Pro501-Glu502-Val503). The highest dissimilarities are detected when considering hKDAC8 characterized by lysine (Lys33) and isoleucine (Ile34) residues, recognized to cause conformational distortion of the binding pocket [48], thus suggesting a role of this sequence in enzyme adaptation.

Sequence 2. Located next to Sequence 1 (**Figure 3C**), this characterizing loop (**Figure 4**, Supplementary material **Figure S4**) has a different primary sequence when considering the four hKDAC isoforms. hKDAC1, 3 and 8 have the most similar amino acid sequence, Gly-X-Asp-Cys, where X is a non-conserved residue represented by a glutamate, aspartate and tyrosine (Glu98, Asp92 and Tyr100), respectively. This difference should affect the hKDAC8 selectivity with respect to the other two isoforms, due to a higher dissimilarity of a tyrosine residue with respect to a glutamate or aspartate. hKDAC6 shows a higher number of non-conserved residues, thus suggesting a different behavior when binding a ligand.

Sequence 3. Located in an inner part of the active site (**Figure 4**, Supplementary material **Figure S4**), below the zinc ion, this sequence is characterized by a conserved leucine residue in hKDAC1 and 3 (Leu139 and Leu133, respectively); while hKDAC6 is characterized by a glycine (Gly609), suggesting recognition of bulkier groups, as a consequence of a decreased steric hindrance. Conversely, the presence of a bulky tryptophan (Trp141) in hKDAC8 hinders access to this portion of the active site channel.

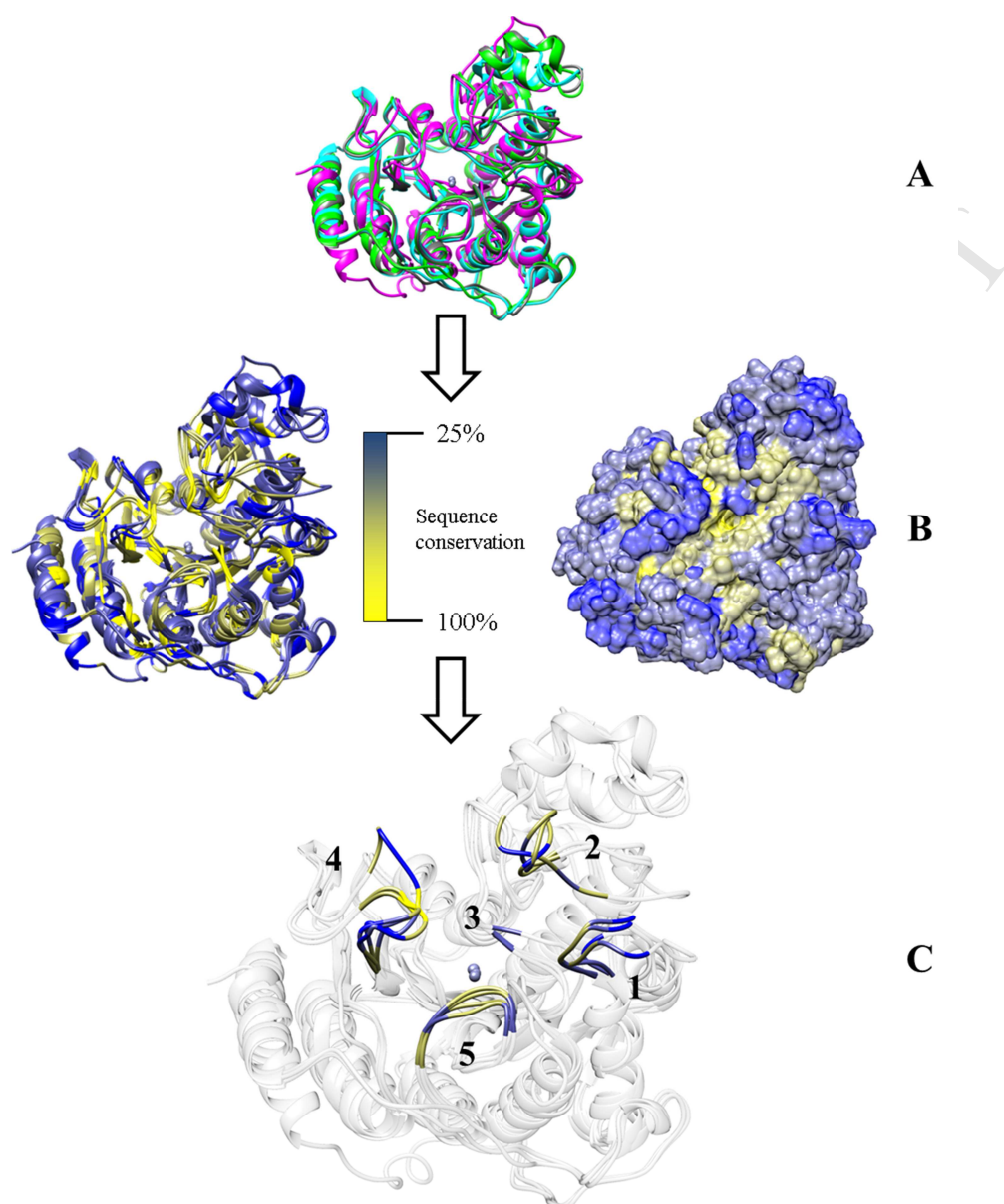


Figure 3. Superimposed hKDAC1 (PDB 4BKX), hKDAC3 (PDB 4A69), hKDAC6 (homology model) and hKDAC8 (PDB 3RQD). The zinc ion is depicted as grey ball. A: hKDAC1 (grey colored), 3 (green colored), 6 (magenta colored) and 8 (cyan colored); B: hKDAC1, 3, 6 and 8 color-coded according to the percentage of conserved residues (gradient color from blue: 25% to yellow: 100%), are depicted as ribbons (left side) and surfaces (right side), respectively. C: highlighted sequences (1 to 5) with lowest residue conservation in the proximity of the active site (see Supplementary material (**Figure S4**) for relative sequences).

Sequence 4. By analyzing this characterizing loop among the four different enzyme isoforms (**Figure 4**, Supplementary material **Figure S4**), a pair of phenylalanine residues is conserved in

hKDACs 3, 6 and 8 (Phe199 and Phe200; Phe679 and Phe680; Phe207 and Phe208, respectively); on the contrary, in hKDAC1 one phenylalanine is replaced by a tyrosine residue (Tyr204). It seems reasonable that the Phe-Phe or Phe-Tyr pairs interact with the linker-cap portions of a hKDAC inhibitor, thus contributing to stabilizing a compound mainly by hydrophobic/steric interactions in the linker or cap regions. The presence of a Tyr204 in hKDAC1 suggests a tendency of hKDAC1 to welcome a more electrostatic interaction (i.e. H-bonds) with respect to the other 3 KDACs. When considering the other residues of sequence 4: starting from those adjacent to the Phe-Phe or Phe-Tyr pair, a proline (Pro206, Pro201, Pro681 and Pro209, in hKDAC 1, 3, 6 and 8 respectively) is conserved, while a glutamate (Glu203), threonine (Thr203), threonine (Thr678) and a glycine (Gly206) characterize the four isoforms (1, 3, 6 and 8 respectively), suggesting a role of these residues in ligand-protein recognition. Differences among other side chains in the loop characterizing this sequence could play a role for conformational adaptation when interacting with a ligand. Another peculiarity of hKDAC6 is the higher number of residues due to an insertion compared to the other isoforms (compare with Supplementary material **Figure S4**), thus suggesting further flexibility of the active site when binding a ligand.

Sequence 5. The characterizing side chains of this segment (**Figure 4**) do not necessarily point towards the active site, but are potentially involved as the size of the ligand increases. The loop is composed by a conserved residue sequence (Arg-Leu-Gly-Cys-Phe) in hKDAC1 and 3, while Pro-Leu-Gly-Gly-Cys in hKDAC6, and Pro-Met-Cys-Ser-Phe in hKDAC8 occur (see Supplementary material **Figure S4**), thus reflecting a different contribution of charged and polar side chains which could determine ligand selectivity.

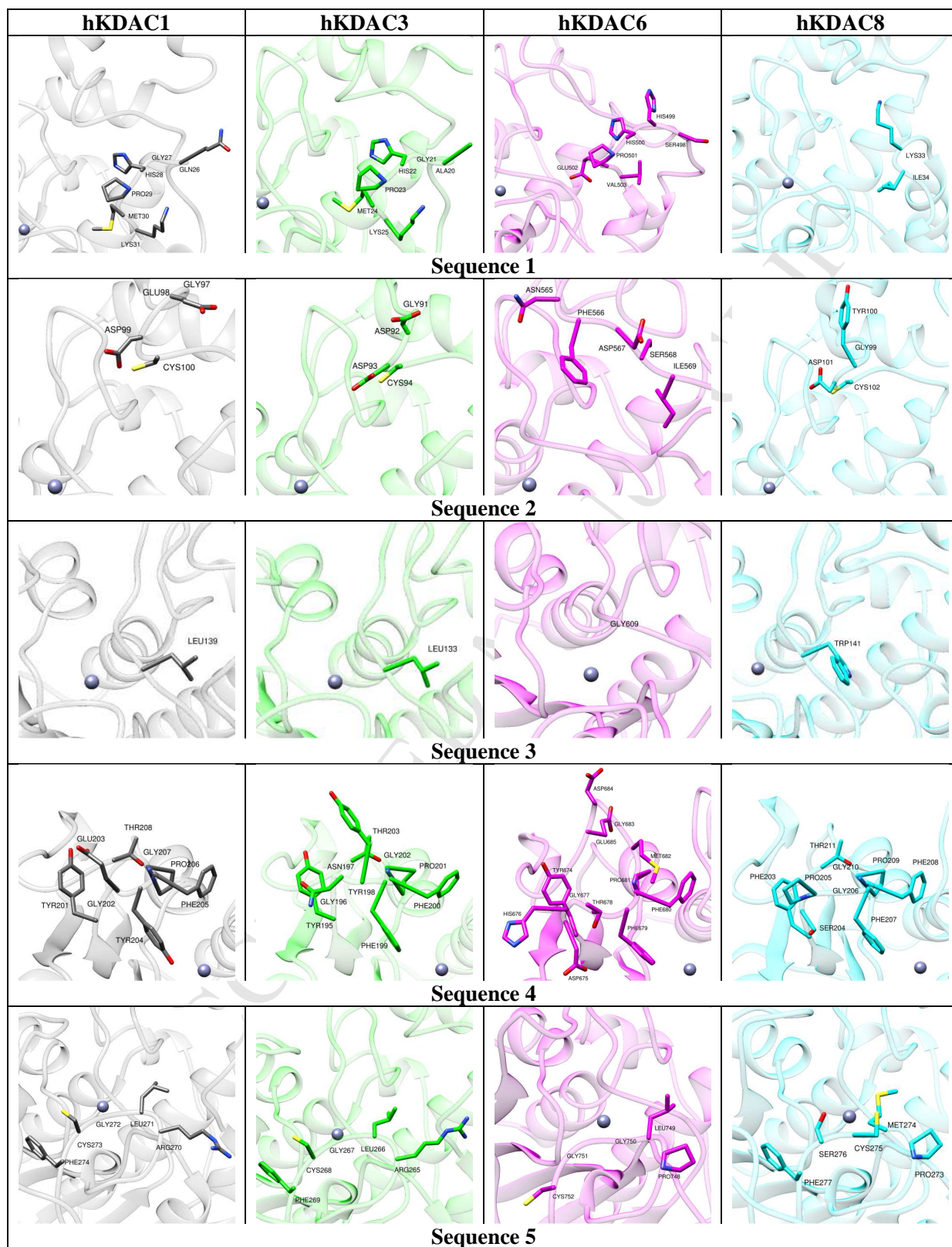


Figure 4. Side chain view of lower conserved sequences close to the active site (1 to 5, **Figure 3C**): hKDAC1 (grey), 3 (green), 6 (magenta) and 8 (cyan). The zinc ion is depicted as grey ball.

Molecular Docking

To rationalize the structure activity relationship of the synthesized 104 BZD derivatives, molecular docking calculations were applied using the four hKDAC isoforms (1, 3, 6 and 8) as target structures.

Docking Assessment. As previously reported [45], a comprehensive docking assessment study has been performed by us (using all the co-crystal hKDAC structures available at the time) to detect the most reliable docking protocol when using the mammalian lysine deacetylases as target. As suggested by the docking assessment results [45], Surflex-Dock [49] was selected to predict the binding poses of the benzodiazepine compounds when the best-docked (BD) [45] poses were considered. A further validation has been performed assuming that every active BZD-hKDACi must interact with the zinc ion (thus having the zinc binding group close to the catalytic ion), conversely for the non-active compounds. Thus, all the best-docked poses obtained from docking the BZD derivatives (**Tables 1 and 2**) were analyzed by correlating the distances between the closest inhibitor's zinc-binding group (ZBG) atom and the zinc ion with the relative biological responses (**Figure 5**). As depicted in **Figure 5**, the docking protocol discriminates the active compounds from the non-active ones among the four enzyme isoforms. In fact, all of the most active BZDs (showing lower IC₅₀ (μM) values) were predicted with the zinc-binding group close to the zinc ion (≈ 2 Å). While for the least active ones (characterized by higher IC₅₀ (μM) or lower inhibition percentage values), the closest inhibitor's atom was progressively farther from the catalytic zinc. The data further confirmed the reliability of the adopted protocol, and the absence of any predicted false negative when considering the BZD derivatives (no BD poses of compounds with an appreciable inhibitory capability were predicted with the ZBG far from the zinc ion).

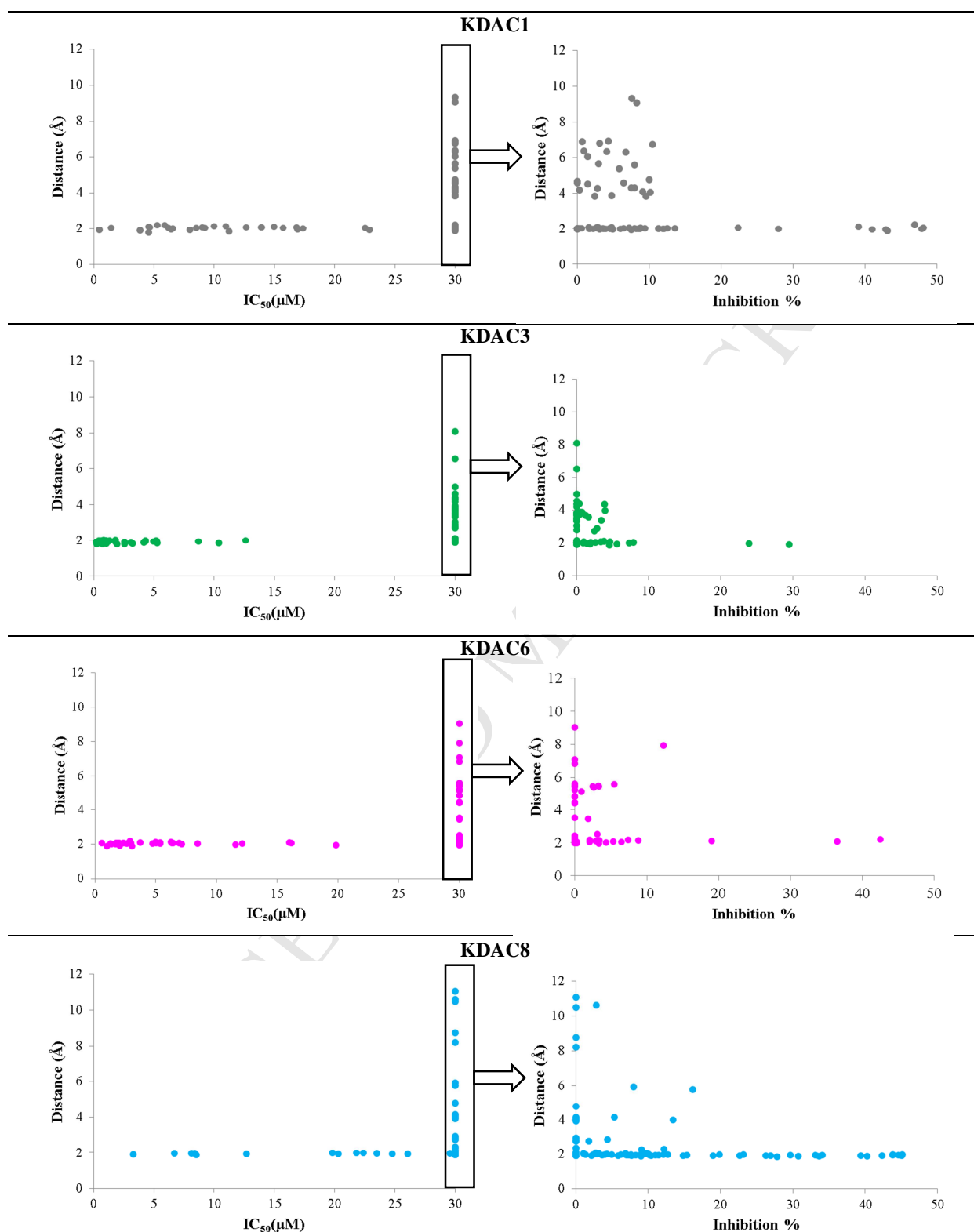


Figure 5. Distances between the zinc ion and the closest BZDs ZBG atoms (y axes) vs the relative biological responses (x axes).

In the case of the hydroxamic acid derivatives, the characteristic bidentate chelation with the zinc ion was generally missed by the docking predictions (see below), as a consequence (from our point of view) of limited protein flexibility and dynamics during the docking simulation, and further magnified by the presence of the large benzodiazepine capping group.

Binding Mode Analysis. As reported above, BZD compound **6h** showed, towards hKDAC1, 3, 6, but not 8, the maximum inhibitory potency among the 104 tested BZDs. Thus, the best docked (BD) [45] poses (**Figure 6**) from each enzyme isoform were investigated to detect those interactions predicted to be necessary for protein recognition when a BZD was present. Beside the importance of a hydroxamic moiety as zinc binding group, a common interaction, between the hydrogen of a zinc-coordinated histidine (His141 in hKDAC1, His172 in hKDAC3, His651 in hKDAC6 and His180 in hKDAC8) and the 2-oxo group of the BZD scaffold was generally detected (**Figure 6**), and judged relevant for the inhibitor potency. As a consequence, a certain length of the linker group (4 carbon atoms generally gave the best results) was necessary to establish a correct 2-oxo group/histidine H-bond interaction. The low selectivity of **6h** among hKDAC1, 3, 6 suggests that the benzodiazepine moiety with a short R₁ group (i.e. a cysteine as pendant amino acid), is indiscriminately well accepted by these series of enzymes and capable to establish a packed network of steric/hydrophobic interactions (mostly with hKDAC3), and steric ones as in hKDAC1 (with Phe205), and hKDAC6 (with Pro748) (see **Figure 6**). On the contrary, **6h** showed low inhibition potency against hKDAC8: by analyzing its docked pose, no particular electrostatic interactions as well as hydrophobic ones were detected, when compared with the other enzyme isoforms. As reported above **6q** showed a similar potency, compared to **6h**, against hKDAC3 and its docked pose suggests the establishment of an H-bond interaction between its pendant amino acid in R₁ (arginine) and the backbone carbonyl oxygen of Tyr198. Since

molecular docking is generally performed using a fixed protein conformation, a direct involvement of the Tyr198 hydroxyl group is plausible with a consequent conformational rearrangement of the characterizing loop (see also sequence 4 in **Figure 4**). Conversely as **6h**, **6q** showed a lower potency against hKDAC1: the predicted docked pose shows an opposite binding conformation of **6q** with respect to **6h** (compare **Figure 7** with **Figure 6**), while an H-bond interaction between the arginine pendant amino acid in R₁ and the backbone's carbonyl group of Glu203 was detected (**Figure 7**). Similarly as reported for hKDAC3, a direct involvement of the Glu203 carboxylate group with a consequent remodeling of the loop (see also sequence 4 in **Figure 4**) is not excluded. The binding pose of **6q** in hKDAC6 is quite similar to the one predicted for **6h** only when considering the benzodiazepine ring, while its pendant amine group (arginine) interacts with the backbone's carbonyl group of a threonine (Thr678, **Figure 7**; see also sequence 4 in **Figure 4**). **6h** (compare **Figure 6** and **8**) suggests a detrimental effect of having positive charged groups interacting with sequence 4 (**Figure 4**). When considering hKDAC8, the predicted conformation of the benzodiazepine moiety characterizing **6q** overlaps that from **6h**, while its arginine guanidinium group interacts with the backbone's carbonyl group of Gly206; this result suggests as anticipated when comparing the different enzyme isoforms (see hKDACs 1, 3, 6 and 8 structures comparisons), the roles of Glu203 (hKDAC1), Tyr198 (hKDAC3), Thr678 (hKDAC6) and Gly206 (hKDAC8) in ligand/protein recognition. Binding mode analysis for those BZDs having the best selectivity by analyzing the GISIndex (**Table 4**), was also performed. Among the first series of compounds showing the highest GISIndex towards hKDAC3 (**6q**, **5d**, **5f**, **5h**, **6p**, **6h**, **5p**, **5l** and **6n**, see Isoform Selectivity paragraph), the first five compound's docked poses were further investigated (**Figure 8**, **6q** was already analyzed above). **5d**, **5f**, **5h** are all characterized by hydrophobic pendant amino acids in R₁ (a leucine, a

methionine and a *tert*-butyl cysteine, respectively), while **6p** has a charged side chain (lysine). Docking calculations predicted all of these compounds bound similarly to hKDAC3 with the different amino acid substituents placed in a region (between Phe199, and Leu266, **Figure 8**) which accepted, preferably, hydrophobic moieties. It should be remarked that an H-bond interaction with Tyr198 seems to guarantee the highest hKDAC3 potency and selectivity (as the case of **6q**). The other series of compounds (**6k**, **11r**), with a detectable selectivity against hKDAC6, are showed in **Figure 9** together with **5k** (which conversely has a poor selectivity between hKDAC3 and 6, **Table 4**). **6k** and **11r** are N1, C3-substituted and C3-substituted derivatives, respectively, and characterized by a similar biological activity against hKDAC6. Their docked poses (**Figure 9**) suggest that the benzodiazepine scaffold establishes hydrophobic/aromatic interactions with Phe566, Gly619, Phe620 and Leu749, while maintaining an H-bond interaction between the 2-oxo group and His651. These interactions appear required for a decent inhibitory activity (in fact the presence of a glutamine as in **6k** doesn't dramatically affect the biological response). **5k** (an N1, C3-substituted BZD) which differs for the presence of a $-(CH_2)_2-CO-NH-Trt$ as group in R_1 shows a similar inhibition potency towards hKDAC3 and 6, confirming the capability for hKDAC6 to accept bulkier moieties. The presence of the Arg673, Asp675 and Arg709 in hKDAC6 (see **5k** in **Figure 9**) could increase the inhibitor selectivity between hKDAC3 and hKDAC6. The most important evidence collected by correlating the BZD chemical structures with the biological responses by molecular modeling are summarized in a pharmacophore scheme (**Figure 10**) as a useful starting point for the development of a next generation of BZD derivatives as hKDACis.

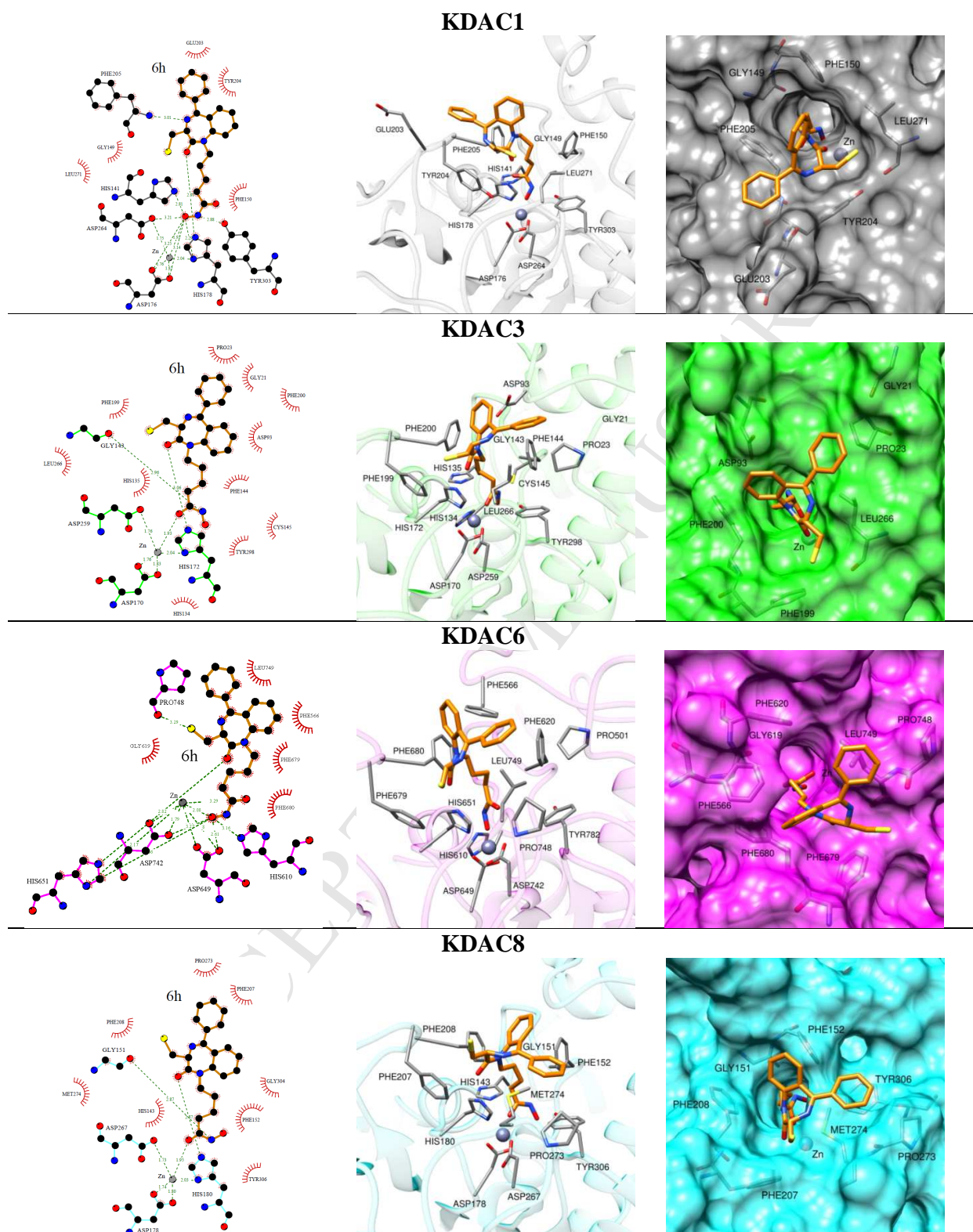


Figure 6. 6h, best docked poses in hKDAC1 (grey colored), 3 (green colored), 6 (magenta colored) and 8 (cyan colored). The zinc ion is depicted as grey ball. From left side to right side: LigPlot+ [50] interaction diagram; active site view; top view.

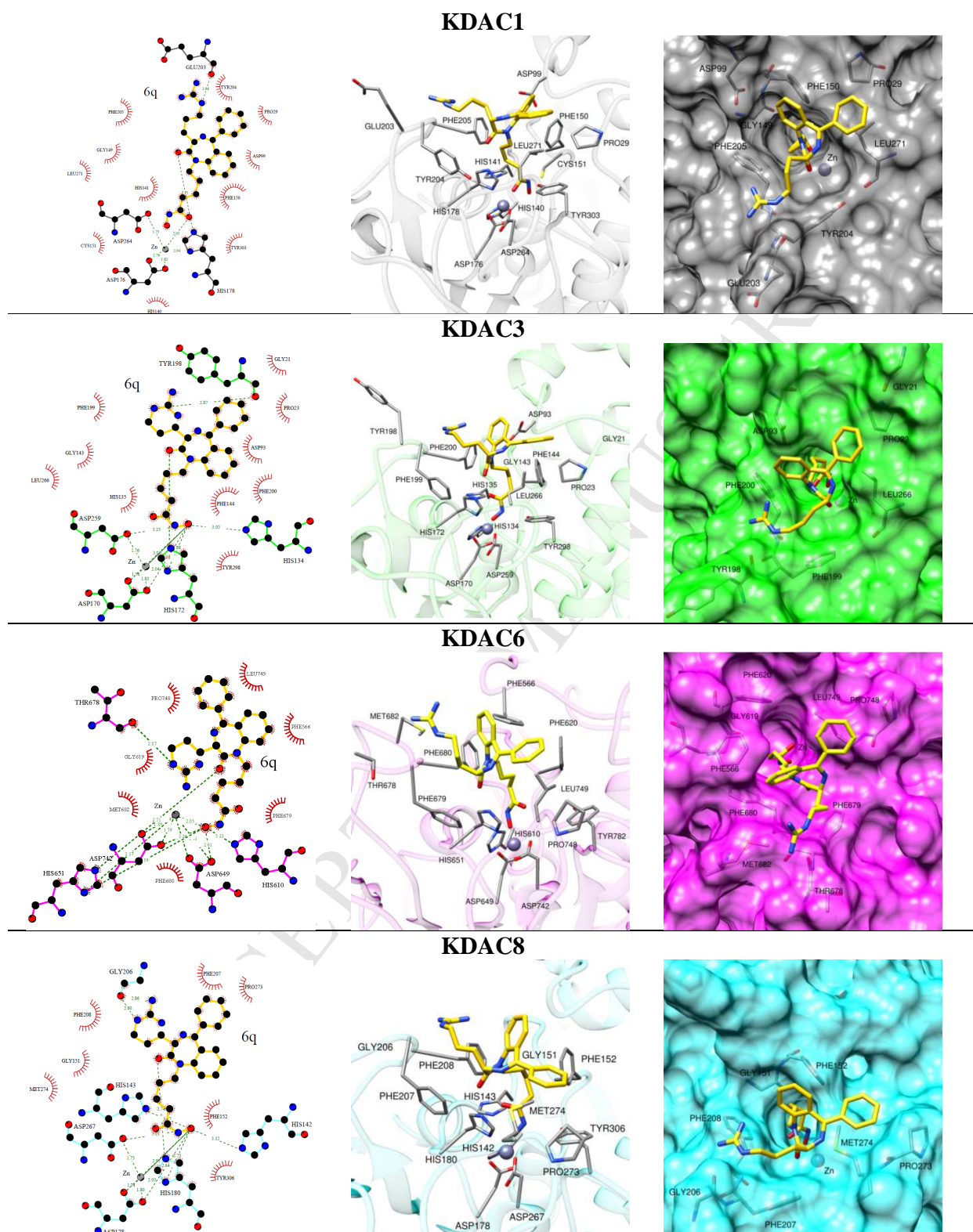


Figure 7. 6q, best docked poses in hKDAC1 (grey colored), 3 (green colored), 6 (magenta colored) and 8 (cyan colored). The zinc ion is depicted as grey ball. From left side to right side: LigPlot+ [50] interaction diagram; active site view; top view.

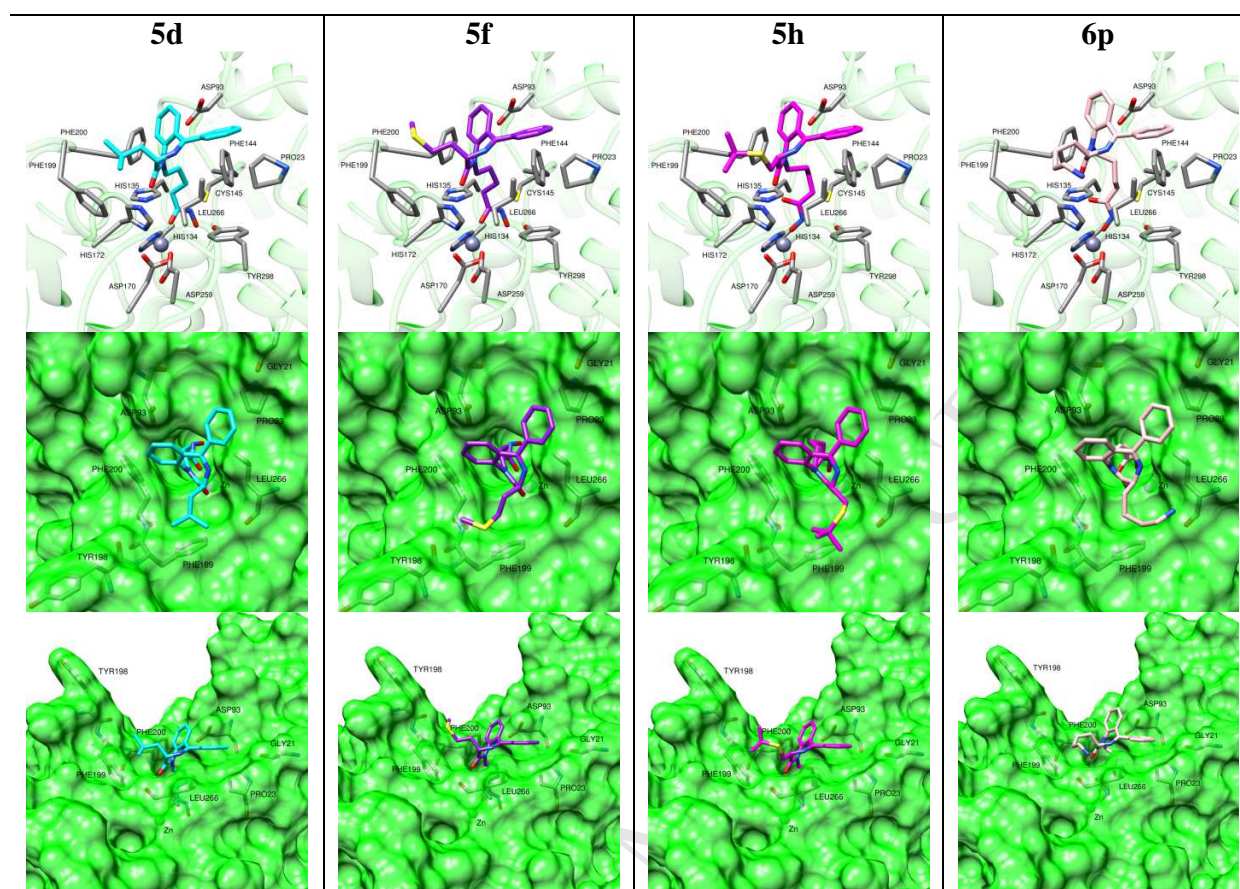


Figure 8. Best docked poses of **5d**, **5f**, **5h** and **6p** in hKDAC3 (green colored): active site view (top); top view (middle); side view (bottom).

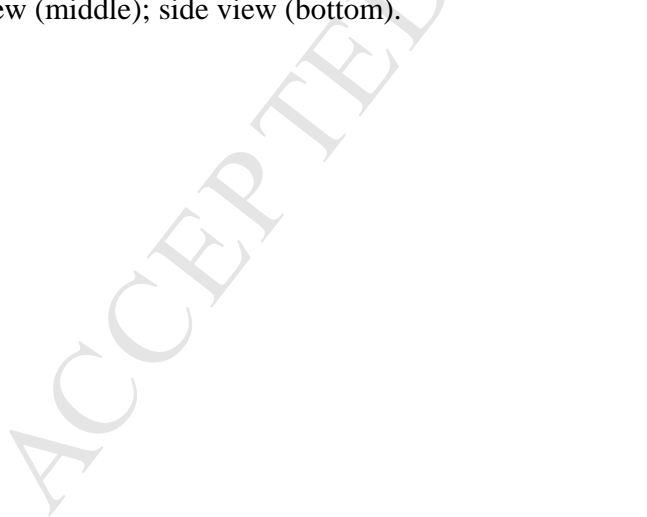


Figure 9. Best docked poses of **5k**, **6k**, **11r** in hKDAC6 (magenta colored): active site view (top); top view (middle); side view (bottom).

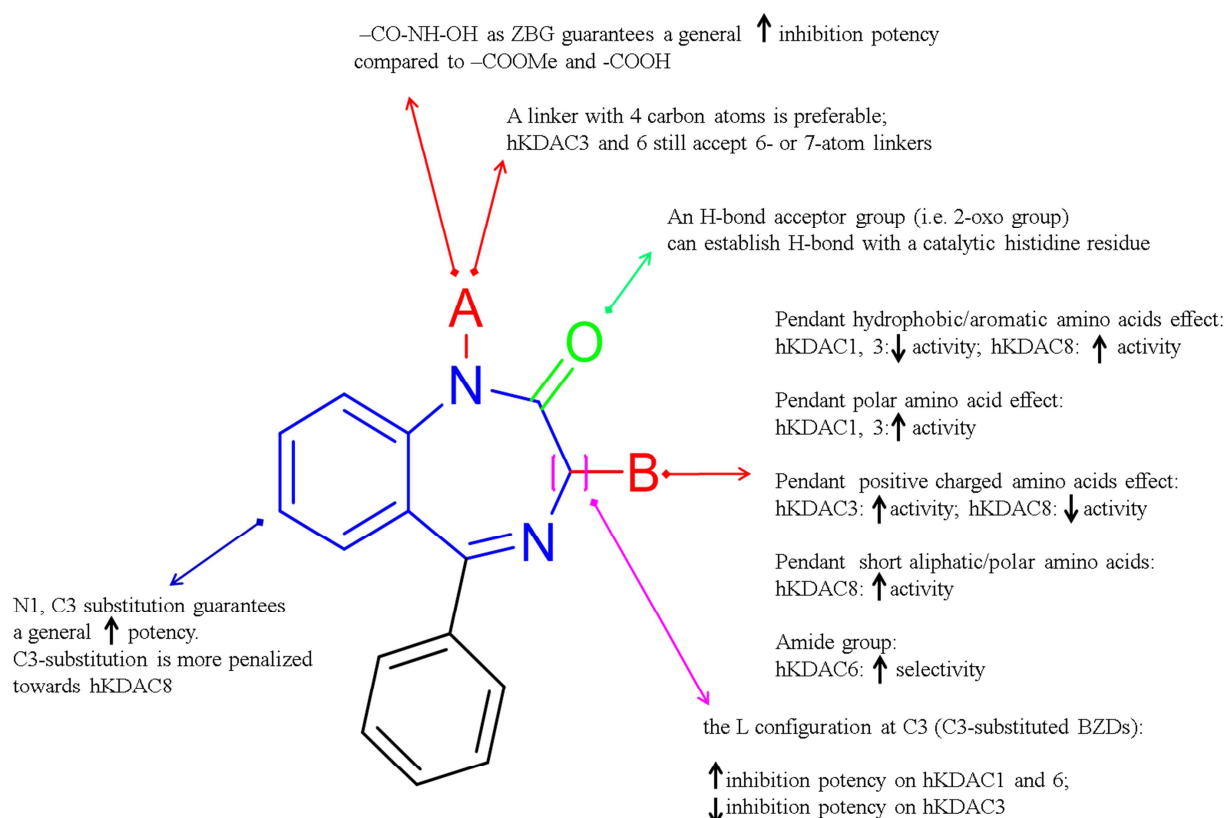


Figure 10. SAR of benzodiazepine derivatives.

CONCLUSIONS

A new class of benzodiazepine derivatives has been designed, synthesized and evaluated for their KDAC isozyme inhibition. Some of the compounds showed class I KDAC selectivity in the inhibition assay against four hKDAC isoforms. In particular, top inhibitor potency (in the mid-nanomolar range) and a promising selectivity were obtained against the hKDAC3 isoform, thus suggesting the benzodiazepine moiety as an interesting lead scaffold for further development to obtain highly potent and selective KDACis. To rationalize the ligand-protein interaction and the impact of the different chemical groups on the biological activity, molecular docking studies were performed by analyzing the best docked poses for the four enzyme isoforms; a homology

model of hKDAC6 was developed and refined by molecular dynamics simulation, thus providing a reliable structure to use for the docking experiments. Structural comparison with a recently released hKDAC6 co-crystal structure (PDB code: 5EDU) confirmed the goodness of the derived homology model. SAR studies, together with the predicted docked poses, allowed rationalization of a BZD-pharmacophore useful for the next development of more potent and selective benzodiazepine derivatives as selective hKDAC inhibitors.

EXPERIMENTAL SECTION

General Information. Starting materials, reagents, and solvents were purchased from commercial vendors unless otherwise noted. ^1H NMR spectra were recorded on a Varian 400 MHz NMR instrument. The chemical shifts were reported as δ ppm relative to TMS using residual solvent peak as the reference unless otherwise noted. The following abbreviations were used to express the multiplicities: s = singlet; d = doublet; t = triplet; q = quartet; m = multiplet; br = broad. High-performance liquid chromatography (HPLC) was carried out on GILSON GX-281 using Waters C18 5 μM , 4.6*50mm and Waters Prep C18 5 μM , 19*150mm reverse phase columns, eluted with a gradient system of 5:95 to 95:5 acetonitrile: water with a buffer consisting of 0.05% TFA. Purity assessment and mass spectra (MS) data were obtained using a Hewlett-Packard HPLC/MSD using electrospray ionization (ESI) for detection. All reactions were monitored by thin layer chromatography (TLC) carried out on Analtech silica gel F plates coated on PE sheets (W/UV254), visualized by using UV (254 nm) or dyes such as ninhydrin, KMnO_4 , *p*-anisaldehyde. The yields shown are not optimized. Flash column chromatography was carried out using 230-400 mesh Selecto Scientific silica gel. All compounds used for biological assays are greater than 95% purity based on HPLC by UV absorbance at 210 nm and 254 nm wavelengths.

Chemistry

General Procedure (A) for the Synthesis of Cyclized Benzodiazepines (BZDs) (2a-2u)

To a stirred solution of BOC/ Fmoc amino acid (**1a-1u**) (1.5 mmol) in THF (15 mL) at -20 °C, NMM (2.25 mmol) and ethylchloroformate (1.5 mmol) were added and the reaction mixture was stirred at -20 °C for 15 min. Later, to this 2-aminobenzophenone (1.5 mmol), NMM (2.25 mmol) were added and stirred at rt for 1-12h. The THF was removed *in vacuo* and the reaction mixture was diluted with ethyl acetate (30 mL) and washed with brine (30 mL), dried (Na₂SO₄), filtered and concentrated under reduced pressure. The crude product (with BOC/ Fmoc) was used in the next step without further purification.

BOC-Deprotection: To a stirred solution of compounds with BOC group in DCM (10 mL) at 0 °C was added TFA (2 mL) and the reaction mixture was stirred at rt for 4-6h. Later, the DCM and TFA were removed under reduced pressure and the crude product was used in the next step without further purification.

Fmoc-Deprotection: To a stirred solution of compounds with Fmoc group in DCM (10 mL) at rt was added piperidine (2 mL) and the reaction mixture was stirred at rt for 0.5-1h. Later, the DCM and piperidine were removed under reduced pressure and the crude product was used in the next step without further purification.

Thereafter, to the resulting BOC/ Fmoc cleaved crude product, ammonium acetate (9.68 mmol) and AcOH (66.73 mmol) were added and the reaction mixture was stirred at rt overnight and then concentrated under reduced pressure to afford an oil. The crude reaction mixture was dissolved in ethyl acetate (30 mL) and washed with saturated NaHCO₃, water (3x40 mL). The organic layer was dried over Na₂SO₄ and filtered. After concentration of the solvent, the crude

product was purified by flash column chromatography using 30-50% EtOAc in hexane (Supplementary material S2).

General Procedure (B) for the Synthesis of *N*-alkylated BZDs (3a-3s)

Cyclized BZD (**2a-2s**) (1.27 mmol) with NaH (2.54 mmol) were stirred in DMF (10 mL) for 1-1.5h under nitrogen. Methyl-5-bromovalerate (1.9 mmol) was added to the reaction mixture, which was stirred for overnight at rt. The DMF was removed *in vacuo* and the reaction mixture was diluted with ethyl acetate (30 mL) and washed with brine (30 mL), dried (Na₂SO₄), filtered and concentrated under reduced pressure. The crude product was purified by flash column chromatography using 30-50% EtOAc in hexane (Supplementary material S2).

General Procedure (C) for the Synthesis of BZD Acids (4a-4q)

To a stirred solution of BZD ester (**3a-3q**) (0.09 mmol) in MeOH (2 mL) was added 1M KOH aqueous solution (to get pH ~9) and stirred at rt for 12h. Later, the MeOH was removed *in vacuo* and the pH was adjusted to 4 with 6N HCl aqueous. The reaction mixture was extracted with EtOAc (3x30 mL), dried (Na₂SO₄), filtered and concentrated under reduced pressure to obtain the BZD acid (**4a-4q**), which was used in the next step without further purification (Supplementary material S2).

General Procedure (D) for the Synthesis of BZD Acids 4r and 4s

To a stirred solution of BZD ester (**3r** or **3s**) (0.54 mmol) in MeOH/ water (9 : 1) was added LiOH (0.81 mmol) and stirred at rt for 12h. Later, the MeOH was removed *in vacuo* and the pH was adjusted to 4 with 1N HCl aqueous. The reaction mixture was extracted with EtOAc (3x30 mL), dried (Na₂SO₄), filtered and concentrated under reduced pressure. The crude product was purified by flash column chromatography using 1-10% MeOH in DCM to afford the pure BZD

acid **4r** or **4s**. Prior to this, the loaded silica in column was treated with 100-200 mL of 0.1% TEA in hexane (Supplementary material S2).

General Procedure (E) for the Synthesis of BZD Hydroxamic Acids (**5a-5s**)

To a stirred solution of BZD acid (**4a-4s**) (0.12 mmol) in THF (6 mL) at -20 °C, NMM (0.18 mmol) and ethylchloroformate (0.12 mmol) were added and the reaction mixture was stirred at -20 °C for 15 min. Later, to this $\text{NH}_2\text{OH}\cdot\text{HCl}$ (0.15 mmol), NMM (0.18 mmol) and few drops of water were added and stirred at rt for 1-12h. The THF was removed *in vacuo* and the reaction mixture was diluted with ethyl acetate (30 mL) and washed with brine (30 mL), dried (Na_2SO_4), filtered and concentrated under reduced pressure. The crude product was purified by flash column chromatography using 1-12% MeOH in DCM. Prior to this, the loaded silica in column was treated with 100-200 mL of 0.1-0.2% TEA in hexane.

General Procedure (F) for the *tBu*, Trt, Pbf and BOC Cleavage on BZD Hydroxamic Acids

The BZD compounds (**5g**, **5m**, **5r**, **5s**, **5n**, **5p**, **5j**, **5k**, **5o**, and **5q**) with *OtBu*, Trt, Pbf and BOC groups were treated with TFA or TFA with 2.5% TIS for 4h at rt. Later, the TFA and TIS were removed *in vacuo* to obtain the BZD hydroxamic acids (**6g**, **6m**, **6r**, **6s**, **6n**, **6p**, **6j**, **6k**, **6o**, and **6q**) free from *tBu*, Trt, Pbf and BOC groups.

1. *N*-hydroxy-5-(2-oxo-5-phenyl-2,3-dihydro-1H-benzo[*e*][1,4]diazepin-1-yl)pentanamide (**5a**)

This BZD hydroxamic acid **5a** was synthesized by using the general procedure **E** employing the BZD acid **4a**. (Yield: 64%) ^1H NMR CDCl_3 + $\text{DMSO}-d_6$: δ 1.2-1.76 (m, 4H), 1.98-2.2 (m, 2H), 3.6-3.8 (m, 2H), 4.78 (s, 2H), 7.18-7.63 (m, 9H), 8.62 (s, 1H). MS (ESI, m/z): found: $[\text{M} + \text{H}]^+$, 352.3, $[\text{M} + \text{Na}]^+$, 375.3, $[2\text{M} + \text{Na}]^+$, 725.5 for $\text{C}_{20}\text{H}_{21}\text{N}_3\text{O}_3$.

2. (S)-N-hydroxy-5-(3-methyl-2-oxo-5-phenyl-2,3-dihydro-1H-benzo[*e*][1,4]diazepin-1-yl)pentanamide (5b)

This BZD hydroxamic acid **5b** was synthesized by using the general procedure **E** employing the BZD acid **4b**. (Yield: 56%) ^1H NMR $\text{CDCl}_3 + \text{DMSO-}d_6$: δ 1.2-1.77 (m, 7H), 1.85-2.05 (m, 2H), 3.57-3.77 (m, 2H), 4.2-4.4 (m, 1H), 7.17-7.6 (m, 9H), 8.8 (s, 1H). MS (ESI, m/z): found: $[\text{M} + \text{H}]^+$, 366.3, $[\text{M} + \text{Na}]^+$, 388.3, $[2\text{M} + \text{Na}]^+$, 753.6 for $\text{C}_{21}\text{H}_{23}\text{N}_3\text{O}_3$.

3. (S)-N-hydroxy-5-(3-isopropyl-2-oxo-5-phenyl-2,3-dihydro-1H-benzo[*e*][1,4]diazepin-1-yl)pentanamide (5c)

This BZD hydroxamic acid **5c** was synthesized by using the general procedure **E** employing the BZD acid **4c**. (Yield: 73%) ^1H NMR CDCl_3 : δ 0.8-1.18 (m, 6H), 1.2-1.8 (m, 4H), 1.81-2.02 (m, 1H), 2.7-2.84 (m, 2H), 3.5-3.65 (m, 2H), 4.2-4.4 (m, 1H), 7.18-7.62 (m, 9H), 8.95 (s, 1H). MS (ESI, m/z): found: $[\text{M} + \text{H}]^+$, 394.4, $[\text{M} + \text{Na}]^+$, 416.4, $[2\text{M} + \text{Na}]^+$, 809.7 for $\text{C}_{23}\text{H}_{27}\text{N}_3\text{O}_3$.

4. (S)-N-hydroxy-5-(3-isobutyl-2-oxo-5-phenyl-2,3-dihydro-1H-benzo[*e*][1,4]diazepin-1-yl)pentanamide (5d)

This BZD hydroxamic acid **5d** was synthesized by using the general procedure **E** employing the BZD acid **4d**. (Yield: 66%) ^1H NMR $\text{CDCl}_3 + \text{DMSO-}d_6$: δ 0.65-1.03 (m, 6H), 1.2-1.78 (m, 3H), 1.8-2.03 (m, 4H), 2.18-2.38 (m, 2H), 3.56-3.7 (m, 2H), 4.2-4.4 (m, 1H), 7.18-7.62 (m, 9H), 8.85 (s, 1H). MS (ESI, m/z): found: $[\text{M} + \text{H}]^+$, 408.4, $[\text{M} + \text{Na}]^+$, 431.4, $[2\text{M} + \text{Na}]^+$, 837.7 for $\text{C}_{24}\text{H}_{29}\text{N}_3\text{O}_3$.

5. 5-((S)-3-((R)-sec-butyl)-2-oxo-5-phenyl-2,3-dihydro-1H-benzo[*e*][1,4]diazepin-1-yl)-N-hydroxypentanamide (5e)

This BZD hydroxamic acid **5e** was synthesized by using the general procedure **E** employing the BZD acid **4e**. (Yield: 48%) ^1H NMR $\text{CDCl}_3 + \text{DMSO}-d_6$: δ 0.78-0.99 (m, 6H), 1.02-1.5 (m, 4H), 1.56-1.79 (m, 2H), 1.81-2.02 (m, 1H), 2.5-2.65 (m, 2H), 3.5-3.7 (m, 2H), 4.2-4.3 (m, 1H), 7.18-7.6 (m, 9H), 9.1 (s, 1H). MS (ESI, m/z): found: $[\text{M} + \text{H}]^+$, 408.4, $[\text{M} + \text{Na}]^+$, 430.4, $[2\text{M} + \text{Na}]^+$, 837.7 for $\text{C}_{24}\text{H}_{29}\text{N}_3\text{O}_3$.

6. (S)-N-hydroxy-5-(3-(2-(methylthio)ethyl)-2-oxo-5-phenyl-2,3-dihydro-1H-benzo[*e*][1,4]diazepin-1-yl)pentanamide (5f)

This BZD hydroxamic acid **5f** was synthesized by using the general procedure **E** employing the BZD acid **4f**. (Yield: 47%) ^1H NMR $\text{CDCl}_3 + \text{DMSO}-d_6$: δ 1.2-1.7 (m, 4H), 2.05 (s, 3H), 2.28-2.58 (m, 4H), 2.6-2.8 (m, 2H), 3.57-3.8 (m, 2H), 4.2-4.4 (m, 1H), 7.18-7.62 (m, 9H), 8.65 (s, 1H). MS (ESI, m/z): found: $[\text{M} + \text{H}]^+$, 426.4, $[\text{M} + \text{Na}]^+$, 448.4, $[2\text{M} + \text{Na}]^+$, 873.7 for $\text{C}_{23}\text{H}_{27}\text{N}_3\text{O}_3\text{S}$.

7. (S)-5-(3-(tert-butoxymethyl)-2-oxo-5-phenyl-2,3-dihydro-1H-benzo[*e*][1,4]diazepin-1-yl)-N-hydroxypentanamide (5g)

This BZD hydroxamic acid **5g** was synthesized by using the general procedure **E** employing the BZD acid **4g**. (Yield: 92%) ^1H NMR $\text{CDCl}_3 + \text{DMSO}-d_6$: δ 1.25 (s, 9H), 1.38-1.7 (m, 4H), 1.9-2.1 (m, 2H), 3.57-3.8 (m, 2H), 3.98-4.04 (m, 2H), 4.25-4.42 (m, 1H), 7.18-7.6 (m, 9H), 8.76 (s, 1H). MS (ESI, m/z): found: $[\text{M} + \text{H}]^+$, 438.4, $[\text{M} + \text{Na}]^+$, 460.5 for $\text{C}_{25}\text{H}_{31}\text{N}_3\text{O}_4$.

8. (S)-5-(3-((tert-butylthio)methyl)-2-oxo-5-phenyl-2,3-dihydro-1H-benzo[*e*][1,4]diazepin-1-yl)-N-hydroxypentanamide (5h)

This BZD hydroxamic acid **5h** was synthesized by using the general procedure **E** employing the BZD acid **4h**. (Yield: 70%) ^1H NMR $\text{CDCl}_3 + \text{DMSO}-d_6$: δ 1.1-1.58 (m, 13H), 1.9-2.02 (m, 2H),

3.3-3.45 (m, 2H), 3.5-3.78 (m, 2H), 4.25-4.4 (m, 1H), 7.18-7.62 (m, 9H), 8.9 (s, 1H). MS (ESI, m/z): found: $[M + H]^+$, 454.4, $[M + Na]^+$, 476.4 for $C_{25}H_{31}N_3O_3S$.

9. 5-((*S*)-3-((*R*)-1-(benzyloxy)ethyl)-2-oxo-5-phenyl-2,3-dihydro-1H-benzo[*e*][1,4]diazepin-1-yl)-N-hydroxypentanamide (5i)

This BZD hydroxamic acid **5i** was synthesized by using the general procedure **E** employing the BZD acid **4i**. (Yield: 54%) 1H NMR $CDCl_3 + DMSO-d_6$: δ 1.3-1.73 (m, 7H), 1.8-2.1 (m, 2H), 3.5-3.65 (m, 2H), 4.2-4.4 (m, 1H), 4.57-4.95 (m, 3H), 7.18-7.62 (m, 14H), 8.65 (s, 1H). MS (ESI, m/z): found: $[M + H]^+$, 486.4, $[M + Na]^+$, 509.4 for $C_{29}H_{31}N_3O_4$.

10. (*S*)-N-hydroxy-5-(2-oxo-3-(2-oxo-2-(tritylamino)ethyl)-5-phenyl-2,3-dihydro-1H-benzo[*e*][1,4]diazepin-1-yl)pentanamide (5j)

This BZD hydroxamic acid **5j** was synthesized by using the general procedure **E** employing the BZD acid **4j**. (Yield: 60%) 1H NMR $CDCl_3 + DMSO-d_6$: δ 0.8-1.6 (m, 4H), 1.9-2.03 (m, 2H), 3.05-3.24 (m, 2H), 3.6-3.8 (m, 2H), 4.2-4.4 (m, 1H), 7.17-7.8 (m, 26H), 9.6 (s, 1H). MS (ESI, m/z): found: $[M + H]^+$, 651.5, $[M + Na]^+$, 674.5 for $C_{41}H_{38}N_4O_4$.

11. (*S*)-N-hydroxy-5-(2-oxo-3-(3-oxo-3-(tritylamino)propyl)-5-phenyl-2,3-dihydro-1H-benzo[*e*][1,4]diazepin-1-yl)pentanamide (5k)

This BZD hydroxamic acid **5k** was synthesized by using the general procedure **E** employing the BZD acid **4k**. (Yield: 76%) 1H NMR $CDCl_3 + DMSO-d_6$: δ 0.8-1.7 (m, 4H), 1.9-2.1 (m, 2H), 2.4-2.62 (m, 4H), 3.6-3.78 (m, 2H), 4.2-4.4 (m, 1H), 6.8-7.6 (m, 24H), 8.82 (s, 1H). MS (ESI, m/z): found: $[M + H]^+$, 665.8, $[M + Na]^+$, 687.8 for $C_{42}H_{40}N_4O_4$.

12. (S)-5-(3-benzyl-2-oxo-5-phenyl-2,3-dihydro-1H-benzo[e][1,4]diazepin-1-yl)-N-hydroxypentanamide (5l)

This BZD hydroxamic acid **5l** was synthesized by using the general procedure **E** employing the BZD acid **4l**. (Yield: 54%) ^1H NMR $\text{CDCl}_3 + \text{DMSO}-d_6$: δ 1.2-1.7 (m, 4H), 1.98-2.1 (m, 2H), 3.5-3.8 (m, 4H), 4.3-4.4 (m, 1H), 7.1-7.6 (m, 14H), 8.65 (s, 1H). MS (ESI, m/z): found: $[\text{M} + \text{H}]^+$, 442.4, $[\text{M} + \text{Na}]^+$, 464.4 for $\text{C}_{27}\text{H}_{27}\text{N}_3\text{O}_3$.

13. (S)-5-(3-(4-(tert-butoxy)benzyl)-2-oxo-5-phenyl-2,3-dihydro-1H-benzo[e][1,4]diazepin-1-yl)-N-hydroxypentanamide (5m)

This BZD hydroxamic acid **5m** was synthesized by using the general procedure **E** employing the BZD acid **4m**. (Yield: 76%) ^1H NMR $\text{CDCl}_3 + \text{DMSO}-d_6$: δ 1.3 (s, 9H), 1.4-1.7 (m, 4H), 1.97-2.1 (m, 2H), 3.5-3.8 (m, 4H), 4.3-4.42 (m, 1H), 6.86-7.6 (m, 13H), 8.7 (s, 1H). MS (ESI, m/z): found: $[\text{M} + \text{H}]^+$, 514.5 for $\text{C}_{31}\text{H}_{35}\text{N}_3\text{O}_4$.

14. tert-butyl (S)-2-((1-(5-(hydroxyamino)-5-oxopentyl)-2-oxo-5-phenyl-2,3-dihydro-1H-benzo[e][1,4]diazepin-3-yl)methyl)-1H-indole-1-carboxylate (5n)

This BZD hydroxamic acid **5n** was synthesized by using the general procedure **E** employing the BZD acid **4n**. (Yield: 88%) ^1H NMR $\text{CDCl}_3 + \text{DMSO}-d_6$: δ 0.8-1.0 (m, 2H), 1.2-1.8 (m, 11H), 1.97-2.1 (m, 2H), 3.57-3.87 (m, 4H), 4.25-4.4 (m, 1H), 7.1-7.65 (m, 13H), 8.1 (s, 1H), 8.82 (s, 1H). MS (ESI, m/z): found: $[\text{M} + \text{H}]^+$, 581.5, $[\text{M} + \text{Na}]^+$, 604.5 for $\text{C}_{34}\text{H}_{36}\text{N}_4\text{O}_5$.

15. (S)-N-hydroxy-5-(2-oxo-5-phenyl-3-((1-trityl-1H-imidazol-5-yl)methyl)-2,3-dihydro-1H-benzo[e][1,4]diazepin-1-yl)pentanamide (5o)

This BZD hydroxamic acid **5o** was synthesized by using the general procedure **E** employing the BZD acid **4o**. (Yield: 38%) ^1H NMR $\text{CDCl}_3 + \text{DMSO}-d_6$: δ 1.1-1.6 (m, 4H), 1.8-2.0 (m, 2H), 3.0-3.58 (m, 2H), 3.6-3.99 (m, 2H), 4.18-4.3 (m, 1H), 6.7-7.6 (m, 26H). MS (ESI, m/z): found: $[\text{M} + \text{H}]^+$, 674.5, $[\text{M} + \text{Na}]^+$, 696.5 for $\text{C}_{43}\text{H}_{39}\text{N}_5\text{O}_3$.

16. tert-butyl (S)-(4-(1-(5-(hydroxyamino)-5-oxopentyl)-2-oxo-5-phenyl-2,3-dihydro-1H-benzo[e][1,4]diazepin-3-yl)butyl)carbamate (5p)

This BZD hydroxamic acid **5p** was synthesized by using the general procedure **E** employing the BZD acid **4p**. (Yield: 70%) ^1H NMR $\text{CDCl}_3 + \text{DMSO}-d_6$: δ 0.8-1.8 (m, 17H), 1.9-2.3 (m, 4H), 3.05-3.23 (m, 2H), 3.4-3.7 (m, 2H), 4.2-4.28 (m, 1H), 4.62 (s, 1H), 7.18-7.6 (m, 9H), 9.15 (s, 1H). MS (ESI, m/z): found: $[\text{M} + \text{H}]^+$, 523.7, $[\text{M} + \text{Na}]^+$, 545.5 for $\text{C}_{29}\text{H}_{38}\text{N}_4\text{O}_5$.

17. (S)-N-hydroxy-5-(2-oxo-3-(3-(3-((2,2,4,6,7-pentamethyl-2,3-dihydrobenzofuran-5-yl)sulfonyl)guanidino)propyl)-5-phenyl-2,3-dihydro-1H-benzo[e][1,4]diazepin-1-yl)pentanamide (5q)

This BZD hydroxamic acid **5q** was synthesized by using the general procedure **E** employing the BZD acid **4q**. (Yield: 47%) ^1H NMR CDCl_3 : δ 0.8-0.99 (m, 2H), 1.2-1.4 (m, 2H), 1.42 (s, 6H), 1.5-1.9 (m, 4H), 2.05 (s, 3H), 2.1-2.38 (m, 4H), 2.5 (s, 3H), 2.58 (s, 3H), 2.96 (s, 2H), 3.2-3.4 (m, 2H), 3.5-3.8 (m, 2H), 4.2-4.38 (m, 1H), 7.1-7.62 (m, 9H). MS (ESI, m/z): found: $[\text{M} + \text{H}]^+$, 703.8, $[\text{M} + \text{Na}]^+$, 725.8 for $\text{C}_{37}\text{H}_{46}\text{N}_6\text{O}_6\text{S}$.

18. tert-butyl (S)-2-(1-(5-(hydroxyamino)-5-oxopentyl)-2-oxo-5-phenyl-2,3-dihydro-1H-benzo[e][1,4]diazepin-3-yl)acetate (5r)

This BZD hydroxamic acid **5r** was synthesized by using the general procedure **E** employing the BZD acid **4r**. (Yield: 71%) ^1H NMR $\text{CDCl}_3 + \text{DMSO}-d_6$: δ 1.2-1.8 (m, 13H), 1.9-2.1 (m, 2H),

3.0-3.4 (m, 2H), 3.6-3.78 (m, 2H), 4.2-4.4 (m, 1H), 7.17-7.6 (m, 9H), 8.7 (s, 1H). MS (ESI, m/z): found: $[M + H]^+$, 466.4 for $C_{26}H_{31}N_3O_5$.

19. *tert*-butyl (S)-3-(1-(5-(hydroxyamino)-5-oxopentyl)-2-oxo-5-phenyl-2,3-dihydro-1H-benzo[*e*][1,4]diazepin-3-yl)propanoate (5s)

This BZD hydroxamic acid **5s** was synthesized by using the general procedure **E** employing the BZD acid **4s**. (Yield: 40%) 1H NMR $CDCl_3$ + DMSO- d_6 : δ 1.4-1.7 (m, 13H), 1.98-2.17 (m, 2H), 2.35-2.6 (m, 4H), 3.59-3.75 (m, 2H), 4.3-4.4 (m, 1H), 7.2-7.6 (m, 9H). MS (ESI, m/z): found: $[M + H]^+$, 480.4 for $C_{27}H_{33}N_3O_5$.

20. (S)-N-hydroxy-5-(3-(hydroxymethyl)-2-oxo-5-phenyl-2,3-dihydro-1H-benzo[*e*][1,4]diazepin-1-yl)pentanamide (6g)

This BZD hydroxamic acid **6g** was synthesized by using the general procedure **F** employing the BZD compound **5g**. (Yield: 86%) 1H NMR $CDCl_3$ + DMSO- d_6 : δ 1.2-1.5 (m, 4H), 2.0-2.1 (m, 2H), 3.6-3.8 (m, 2H), 4.1-4.2 (m, 2H), 4.22-4.43 (m, 1H), 7.18-7.63 (m, 9H), 12.2 (s, 1H). MS (ESI, m/z): found: $[M + H]^+$, 382.4, $[M + Na]^+$, 404.4 for $C_{21}H_{23}N_3O_4$.

21. (S)-N-hydroxy-5-(3-(mercaptomethyl)-2-oxo-5-phenyl-2,3-dihydro-1H-benzo[*e*][1,4]diazepin-1-yl)pentanamide (6h)

Compound **5h** (0.03 mmol) and trifluoromethanesulfonic acid (1.5 mL) were stirred at rt for 4h. Later the reaction mixture was quenched on ice and extracted with ethyl acetate, dried (Na_2SO_4), filtered and concentrated under reduced pressure. The crude product was purified by preparative RP-HPLC to afford the pure BZD hydroxamate **6h** in 10% yield. MS (ESI, m/z): found: $[M + H]^+$, 398.3, $[M + Na]^+$, 420.4 for $C_{21}H_{23}N_3O_3S$.

22. N-hydroxy-5-((S)-3-((R)-1-hydroxyethyl)-2-oxo-5-phenyl-2,3-dihydro-1H-benzo[e][1,4]diazepin-1-yl)pentanamide (6i)

To a stirred solution of benzylated BZD **5i** (0.035 mmol) in DCM (2 mL) at rt was added excess of $\text{BF}_3 \cdot \text{OEt}_2$ (0.7 mmol) and EtSH (0.7 mmol). The reaction mixture was stirred at rt for 6h and purified by preparative RP-HPLC to afford the pure BZD **6i** in 20% yield. ^1H NMR CDCl_3 + DMSO-d_6 : δ 1.2-1.7 (m, 7H), 1.9-2.2 (m, 2H), 3.5-3.8 (m, 2H), 4.22-4.42 (m, 1H), 4.58-4.68 (m, 3H), 7.23-7.8 (m, 9H). MS (ESI, m/z): found: $[\text{M} + \text{H}]^+$, 396.4 for $\text{C}_{22}\text{H}_{25}\text{N}_3\text{O}_4$.

23. (S)-5-(3-(2-amino-2-oxoethyl)-2-oxo-5-phenyl-2,3-dihydro-1H-benzo[e][1,4]diazepin-1-yl)-N-hydroxypentanamide (6j)

This BZD hydroxamic acid **6j** was synthesized by using the general procedure **F** employing the BZD compound **5j**. (Yield: 75%) ^1H NMR CDCl_3 + DMSO-d_6 : δ 1.2-1.7 (m, 4H), 1.98-2.1 (m, 2H), 3.0-3.3 (m, 2H), 3.65-3.8 (m, 2H), 4.2-4.4 (m, 1H), 6.03 (m, 2H), 7.0-7.7 (m, 9H). MS (ESI, m/z): found: $[\text{M} + \text{H}]^+$, 409.4, $[\text{M} + \text{Na}]^+$, 431.3 for $\text{C}_{22}\text{H}_{24}\text{N}_4\text{O}_4$.

24. (S)-5-(3-(3-amino-3-oxopropyl)-2-oxo-5-phenyl-2,3-dihydro-1H-benzo[e][1,4]diazepin-1-yl)-N-hydroxypentanamide (6k)

This BZD hydroxamic acid **6k** was synthesized by using the general procedure **F** employing the BZD compound **5k**. (Yield: 78%) ^1H NMR CDCl_3 + DMSO-d_6 : δ 0.8-1.68 (m, 4H), 2.05-2.2 (m, 2H), 2.38-2.6 (m, 4H), 3.6-3.8 (m, 2H), 4.2-4.4 (m, 1H), 5.7 (s, 2H), 6.45 (s, 2H), 7.0-7.6 (m, 9H). MS (ESI, m/z): found: $[\text{M} + \text{H}]^+$, 423.4, $[\text{M} + \text{Na}]^+$, 445.4 for $\text{C}_{23}\text{H}_{26}\text{N}_4\text{O}_4$.

25. (S)-N-hydroxy-5-(3-(4-hydroxybenzyl)-2-oxo-5-phenyl-2,3-dihydro-1H-benzo[e][1,4]diazepin-1-yl)pentanamide (6m)

This BZD hydroxamic acid **6m** was synthesized by using the general procedure **F** employing the BZD compound **5m**. (Yield: 90%) ^1H NMR $\text{CDCl}_3 + \text{DMSO}-d_6$: δ 1.2-1.4 (m, 4H), 2.2-2.4 (m, 2H), 3.1-3.3 (m, 4H), 4.8-5.0 (m, 1H), 6.7-7.6 (m, 13H), 12.2 (s, 1H). MS (ESI, m/z): found: $[\text{M} + \text{H}]^+$, 458.4 for $\text{C}_{27}\text{H}_{27}\text{N}_3\text{O}_4$.

26. (S)-5-(3-((1H-indol-2-yl)methyl)-2-oxo-5-phenyl-2,3-dihydro-1H-benzo[*e*][1,4]diazepin-1-yl)-N-hydroxypentanamide (6n)

This BZD hydroxamic acid **6n** was synthesized by using the general procedure **F** employing the BZD compound **5n**. (Yield: 60%) ^1H NMR $\text{CDCl}_3 + \text{DMSO}-d_6$: δ 1.18-1.6 (m, 4H), 1.9-2.04 (m, 2H), 3.58-3.8 (m, 4H), 4.25-4.4 (m, 1H), 6.97-7.62 (m, 14H), 9.97 (s, 1H). MS (ESI, m/z): found: $[\text{M} + \text{H}]^+$, 481.4, $[\text{M} + \text{Na}]^+$, 503.4 for $\text{C}_{29}\text{H}_{28}\text{N}_4\text{O}_3$.

27. (S)-5-(3-((1H-imidazol-5-yl)methyl)-2-oxo-5-phenyl-2,3-dihydro-1H-benzo[*e*][1,4]diazepin-1-yl)-N-hydroxypentanamide (6o)

This BZD hydroxamic acid **6o** was synthesized by using the general procedure **F** employing the BZD compound **5o**. (Yield: 56%) ^1H NMR $\text{CDCl}_3 + \text{DMSO}-d_6$: δ 1.15-1.6 (m, 4H), 1.85-2.0 (m, 2H), 3.05-3.6 (m, 2H), 3.61-3.98 (m, 2H), 4.2-4.4 (m, 1H), 7.05-7.83 (m, 11H), 8.65 (s, 1H), 10.2 (s, 1H). MS (ESI, m/z): found: $[\text{M} + \text{H}]^+$, 432.4, $[\text{M} + \text{Na}]^+$, 454.4 for $\text{C}_{24}\text{H}_{25}\text{N}_5\text{O}_3$.

28. (S)-5-(3-(4-aminobutyl)-2-oxo-5-phenyl-2,3-dihydro-1H-benzo[*e*][1,4]diazepin-1-yl)-N-hydroxypentanamide (6p)

This BZD hydroxamic acid **6p** was synthesized by using the general procedure **F** employing the BZD compound **5p**. (Yield: 85%) ^1H NMR $\text{CDCl}_3 + \text{DMSO}-d_6$: δ 1.2-1.8 (m, 8H), 2.0-2.2 (m, 2H), 2.3-2.4 (m, 2H), 3.05-3.2 (m, 2H), 3.4-3.58 (m, 2H), 3.8-4.1 (m, 1H), 7.18-7.63 (m, 9H),

8.2 (s, 1H), 12.1 (s, 1H). MS (ESI, m/z): found: $[M + H]^+$, 423.4, $[M + Na]^+$, 445.4 for $C_{24}H_{30}N_4O_3$.

29. (S)-5-(3-(3-guanidinopropyl)-2-oxo-5-phenyl-2,3-dihydro-1H-benzo[*e*][1,4]diazepin-1-yl)-N-hydroxypentanamide (6q)

This BZD hydroxamic acid **6q** was synthesized by using the general procedure **F** employing the BZD compound **5q**, and purified by preparative RP-HPLC to obtain the pure compound **6q**. (Yield: 13%) 1H NMR $CDCl_3 + DMSO-d_6$: δ 1.38-1.9 (m, 6H), 2.0-2.37 (m, 4H), 2.6 (s, 1H), 3.4-3.8 (m, 4H), 4.22-4.39 (m, 1H), 6.8-7.8 (m, 13H). MS (ESI, m/z): found: $[M + H]^+$, 451.4 for $C_{24}H_{30}N_6O_3$.

30. (S)-2-(1-(5-(hydroxyamino)-5-oxopentyl)-2-oxo-5-phenyl-2,3-dihydro-1H-benzo[*e*][1,4]diazepin-3-yl)acetic acid (6r)

This BZD hydroxamic acid **6r** was synthesized by using the general procedure **F** employing the BZD compound **5r**. (Yield: 91%) 1H NMR $CDCl_3 + DMSO-d_6$: δ 1.38-1.7 (m, 4H), 1.9-2.1 (m, 2H), 3.0-3.4 (m, 2H), 3.9-4.1 (m, 2H), 4.2-4.4 (m, 1H), 7.18-7.8 (m, 10H). MS (ESI, m/z): found: $[M + H]^+$, 410.3, $[M + Na]^+$, 432.3 for $C_{22}H_{23}N_3O_5$.

31. (S)-3-(1-(5-(hydroxyamino)-5-oxopentyl)-2-oxo-5-phenyl-2,3-dihydro-1H-benzo[*e*][1,4]diazepin-3-yl)propanoic acid (6s)

This BZD hydroxamic acid **6s** was synthesized by using the general procedure **F** employing the BZD compound **5s**. (Yield: 83%) 1H NMR $CDCl_3 + DMSO-d_6$: δ 1.2-1.6 (m, 4H), 1.9-2.1 (m, 2H), 2.3-2.63 (m, 4H), 3.6-3.75 (m, 2H), 4.2-4.4 (m, 1H), 7.18-7.63 (m, 9H). MS (ESI, m/z): found: $[M + H]^+$, 424.4, $[M + Na]^+$, 446.4 for $C_{23}H_{25}N_3O_5$.

32. (S)-N-hydroxy-2-(2-oxo-5-phenyl-2,3-dihydro-1H-benzo[e][1,4]diazepin-3-yl)acetamide (8r)

This BZD hydroxamic acid **8r** was synthesized by using the general procedure **E** employing the BZD acid **7r**. (Yield: 46%) ^1H NMR $\text{CDCl}_3 + \text{DMSO-d}_6$: δ 2.99-3.19 (m, 2H), 4.1-4.22 (m, 1H), 7.03-7.6 (m, 9H), 8.2 (s, 1H), 9.5 (s, 1H), 9.85 (s, 1H). MS (ESI, m/z): found: $[\text{M} + \text{H}]^+$, 310.3, $[\text{M} + \text{Na}]^+$, 332.3, $[2\text{M} + \text{Na}]^+$, 641.4 for $\text{C}_{17}\text{H}_{15}\text{N}_3\text{O}_3$.

33. (S)-N-hydroxy-3-(2-oxo-5-phenyl-2,3-dihydro-1H-benzo[e][1,4]diazepin-3-yl)propanamide (8s)

This BZD hydroxamic acid **8s** was synthesized by using the general procedure **E** employing the BZD acid **7s**. (Yield: 32%) ^1H NMR $\text{CDCl}_3 + \text{DMSO-d}_6$: δ 2.2-2.6 (m, 4H), 3.57-3.7 (m, 1H), 7.0-7.59 (m, 9H), 9.28 (s, 1H), 9.9 (s, 1H). MS (ESI, m/z): found: $[\text{M} + \text{H}]^+$, 324.3, $[\text{M} + \text{Na}]^+$, 346.3, $[2\text{M} + \text{Na}]^+$, 669.5 for $\text{C}_{18}\text{H}_{17}\text{N}_3\text{O}_3$.

34. (R)-N-hydroxy-2-(2-oxo-5-phenyl-2,3-dihydro-1H-benzo[e][1,4]diazepin-3-yl)acetamide (8t)

This BZD hydroxamic acid **8t** was synthesized by using the general procedure **E** employing the BZD acid **7t**. (Yield: 55%) ^1H NMR $\text{CDCl}_3 + \text{DMSO-d}_6$: δ 2.9-3.2 (m, 2H), 4.1-4.23 (m, 1H), 7.02-7.6 (m, 9H), 8.18 (s, 1H), 9.46 (s, 1H), 9.85 (s, 1H). MS (ESI, m/z): found: $[\text{M} + \text{H}]^+$, 310.3, $[\text{M} + \text{Na}]^+$, 332.3, $[2\text{M} + \text{Na}]^+$, 641.5 for $\text{C}_{17}\text{H}_{15}\text{N}_3\text{O}_3$.

35. (R)-N-hydroxy-3-(2-oxo-5-phenyl-2,3-dihydro-1H-benzo[e][1,4]diazepin-3-yl)propanamide (8u)

This BZD hydroxamic acid **8u** was synthesized by using the general procedure **E** employing the BZD acid **7u**. (Yield: 23%) ^1H NMR $\text{CDCl}_3 + \text{DMSO}-d_6$: δ 1.98-2.2 (m, 2H), 2.3-2.6 (m, 2H), 3.58-3.7 (m, 1H), 7.0-7.6 (m, 9H), 8.4 (s, 1H), 9.77 (s, 1H), 10.02 (s, 1H). MS (ESI, m/z): found: $[\text{M} + \text{H}]^+$, 324.3, $[\text{M} + \text{Na}]^+$, 346.3, $[2\text{M} + \text{Na}]^+$, 669.5 for $\text{C}_{18}\text{H}_{17}\text{N}_3\text{O}_3$.

36. (S)-N-hydroxy-4-(2-(2-oxo-5-phenyl-2,3-dihydro-1H-benzo[e][1,4]diazepin-3-yl)acetamido)butanamide (11r)

This BZD hydroxamic acid **11r** was synthesized by using the general procedure **E** employing the BZD acid **10r**. (Yield: 45%) ^1H NMR $\text{CDCl}_3 + \text{DMSO}-d_6$: 1.2-1.38 (m, 2H), 1.8-2.0 (m, 2H), 2.3-2.5 (m, 2H), 2.95-3.24 (m, 2H), 4.1-4.22 (m, 1H), 7.03-7.6 (m, 10H), 9.58 (s, 1H). MS (ESI, m/z): found: $[\text{M} + \text{H}]^+$, 395.4, $[\text{M} + \text{Na}]^+$, 418.4 for $\text{C}_{21}\text{H}_{22}\text{N}_4\text{O}_4$.

37. (S)-N-hydroxy-4-(3-(2-oxo-5-phenyl-2,3-dihydro-1H-benzo[e][1,4]diazepin-3-yl)propanamido)butanamide (11s)

This BZD hydroxamic acid **11s** was synthesized by using the general procedure **E** employing the BZD acid **10s**. (Yield: 50%) ^1H NMR $\text{CDCl}_3 + \text{DMSO}-d_6$: 1.6-1.8 (m, 2H), 1.9-2.05 (m, 2H), 2.3-2.6 (m, 2H), 3.0-3.2 (m, 2H), 3.21-3.4 (m, 2H), 3.8-4.0 (m, 1H), 7.1-7.78 (m, 10H), 8.02 (s, 1H), 10.2 (s, 1H), 11.3 (s, 1H). MS (ESI, m/z): found: $[\text{M} + \text{H}]^+$, 409.4, $[\text{M} + \text{Na}]^+$, 431.4 for $\text{C}_{22}\text{H}_{24}\text{N}_4\text{O}_4$.

38. (S)-N-hydroxy-5-(3-(2-(hydroxyamino)-2-oxoethyl)-2-oxo-5-phenyl-2,3-dihydro-1H-benzo[e][1,4]diazepin-1-yl)pentanamide (13r)

This BZD hydroxamic acid **13r** was synthesized by using the general procedure **E** employing the BZD acid **12r**. (Yield: 20%) ^1H NMR $\text{CDCl}_3 + \text{DMSO}-d_6$: δ 1.2-1.6 (m, 4H), 2.4-2.63 (m, 2H),

2.8-3.03 (m, 2H), 3.18-3.5 (m, 2H), 3.9-4.3 (m, 1H), 7.2-7.6 (m, 9H), 12.7 (s, 2H). MS (ESI, m/z): found: $[M + H]^+$, 425.4, $[M + Na]^+$, 447.4 for $C_{22}H_{24}N_4O_5$.

39. (S)-N-hydroxy-5-(3-(3-(hydroxyamino)-3-oxopropyl)-2-oxo-5-phenyl-2,3-dihydro-1H-benzo[*e*][1,4]diazepin-1-yl)pentanamide (13s)

This BZD hydroxamic acid **13s** was synthesized by using the general procedure **E** employing the BZD acid **12s**. (Yield: 31%) 1H NMR $CDCl_3$ + $DMSO-d_6$: δ 1.2-1.6 (m, 4H), 1.9-2.2 (m, 2H), 2.22-2.45 (m, 4H), 3.58-3.7 (m, 2H), 4.1-4.3 (m, 1H), 7.0-7.8 (m, 9H), 9.9 (s, 1H), 10.1 (s, 1H). MS (ESI, m/z): found: $[M + H]^+$, 439.4 for $C_{23}H_{26}N_4O_5$.

Microfluidic chip-based KDAC inhibition assay

Four different substrates were used according to the hKDAC isoform: 1) a (FAM)-labeled peptide purchasable from PerkinElmer (Broad Substrate A, Product number CLS960006), was synthesized in house as previously reported [35] and used for hKDAC1 assays; 2) two (FITC)-labeled peptides were purchased from PerkinElmer (p53 Acetylated Peptide and Histone 4 Acetylated Peptide, Product Number 760512 and 760513 respectively) and used as substrates to test compounds against hKDAC 3 and 6, respectively; 3) a (FAM)-labeled peptide (Broad Substrate B, Product Number CLS960007) was employed as substrate for hKDAC8 assays. All hKDACs were purchased from BPS Bioscience. Compounds were tested using two replicates in a 10-point dose curve with 3-fold serial dilution starting from 30 μM . Purified hKDACs were incubated with 1 μM of substrate and BZDs for 60 min at room temperature in KDAC assay buffer that contained 25 mM Tris-HCl (pH 8.0), 137 mM NaCl, 2.7 mM KCl, 1 mM $MgCl_2$, and 0.01% BSA. Reactions (using two replicates) were terminated by the addition of a stop buffer containing 100 mM HEPES, 0.015% Brij-35, 10 mM EDTA, 0.1% CR-3 and 1.5 μM of the

known pan-KDAC inhibitor Panobinostat [23, 24]. Fluorescence intensity of electrophoretically separated substrate and product was detected using the Labchip EZ Reader and the data were analyzed by non-linear regression using GraphPad Prism 6.01 software [51] to afford IC₅₀ values from dose-response experiments. The percentage of inhibition at 30 μ M is reported when its value is less than 50% at that concentration. As standard compounds (positive controls), ten well-known KDAC inhibitors (see **Table 3**) were used: Entinostat (MS-275) [36], TSA [40], Tubastatin A [41], SAHA [43], (all purchased from Selleck Chemicals), an α -amino-ketone derivative originally named compound **4** [44] (synthesized in house), LBH589 [23, 24] (purchased from ApexBio Technology), PCI-34051 [38] (purchased from Cayman Chemical Company), T247 [42] (synthesized in house as previously reported) [35], largazole [52] (thioester) and one of its analog (herein designated SD-L-256 [39], were generously supplied by Prof. Robert Williams of the Department of Chemistry at Colorado State University).

Molecular Modeling

hKDACs 1, 3 and 8 complex structures preparation

Crystal structures of hKDAC1, hKDAC3, and hKDAC8 (PDB codes 4BKX, 4A69, 3RQD, respectively) were retrieved from the Protein Data Bank (PDB), [53] and then prepared as previously reported [45]; briefly: 1) all solvent molecules, buffer and non-interacting ions were removed, then hydrogens were added considering a neutral pH (pH=7.4); 2) non-terminal missing residues were rebuilt by using MODELLER 9.14 program [54]; 3) a final energy minimization has been performed by means of the GROMACS 5.0.2 [55].

hKDAC6 MD Simulations

GROMACS 5.0.2 [55] has been used. The AMBER99SB-ILDN [56] force field with TIP4P [57] as the water model was adopted, while Na^+ counter-ions were used to neutralize the system. A first equilibration under a NVT (constant number of particles, volume and temperature) ensemble at 300K over a period of 100 ps was performed; subsequently, the system has been submitted to a 100 ps NPT (constant number of particles, pressure and temperature) equilibration. Both NVT and NPT equilibrations have been performed with positional restraints to the ligand atoms. The equilibrated structure was then submitted to a 95 ns unrestrained MD.

Preparation of BZDs Minimized Random Conformations

To generate ligands random conformations, used as starting conformation to use for molecular docking, the OpenBabel suite (The Open Babel package, version 2.3.2 <http://openbabel.org>) [58] was firstly used to: assign the protonation states at pH 7.4; generate a best conformer (after 250 geometry optimization steps) out of 250 conformers using the obconformer tool. Then a further optimization of the obtained geometry has been performed by means of the obminimize tool (using first the steepest descent algorithm followed by the conjugate gradients algorithm with a default number of steps and force-field).

Molecular Docking

Surflex-Dock [49] version 2.745 was used for molecular docking calculations using the same settings as previously reported [45]. Best docked poses were extrapolated using the Clusterizer [45] software and a in house script has been used to compute and collect the distance (in Å) between the zinc ion and the closest ZBG atom of each ligand.

SUPPLEMENTARY MATERIAL

Detailed experimental procedures and spectral characterization data of compounds, inhibitory percentages, IC₅₀ values, dose-response curves, selectivity indexes, MD simulation results, hKDACs 1, 3, 6 and 8 superimposed sequences, hKDAC6 homology model.

CORRESPONDING AUTHOR

Garland R. Marshall; E-mail: garlandm@gmail.com; phone: +1-314-362-6039

FUNDING SOURCES

This work was supported by the National Institutes of Health (NIH, grant number 5R01GM106974).

ABBREVIATIONS USED

AcOH, acetic acid; BD, best docked poses; BZD, benzodiazepine; ECF, ethyl chloroformate; EtOAc, ethyl acetate; EtSH, ethanethiol; FITC, fluoresceine isothiocyanate; GISIndex, global isoform selectivity index; HA_RMSD_h, hungarian symmetry-corrected heavy-atom RMSD; hKDAC, human lysine deacetylase; KDACi, lysine deacetylase inhibitor; MD, molecular dynamics; MeOH, methanol; NMM, *N*-methylmorpholine; PDB, protein data bank; RCRD, random conformation re-docking; RMSD, root mean squared deviation; SAHA, suberoyl anilide hydroxamic acid; SI, selectivity index; TEA, triethylamine; TSA, trichostatin A; TIS, triisopropylsilane; ZBG, zinc binding group.

REFERENCES

- [1] S. Minucci, P.G. Pelicci, Histone deacetylase inhibitors and the promise of epigenetic (and more) treatments for cancer, *Nat. Rev. Cancer* 6 (2006) 38-51.
- [2] K.J. Falkenberg, R.W. Johnstone, Histone deacetylases and their inhibitors in cancer, neurological diseases and immune disorders, *Nat. Rev. Drug Discovery* 13 (2014) 673-691.
- [3] J.E. Bolden, M.J. Peart, R.W. Johnstone, Anticancer activities of histone deacetylase inhibitors, *Nat. Rev. Drug Discovery* 5 (2006) 769-784.
- [4] W. Weichert, HDAC expression and clinical prognosis in human malignancies, *Cancer Lett.* 280 (2009) 168-176.
- [5] O. Khan, N.B. La Thangue, HDAC inhibitors in cancer biology: emerging mechanisms and clinical applications, *Immunol. Cell Biol.* 90 (2012) 85-94.
- [6] N. Gammoh, D. Lam, C. Puente, I. Ganley, P.A. Marks, X. Jiang, Role of autophagy in histone deacetylase inhibitor-induced apoptotic and nonapoptotic cell death, *Proc. Natl. Acad. Sci. U.S.A.* 109 (2012) 6561-6565.
- [7] E. Verdin, F. Dequiedt, H.G. Kasler, Class II histone deacetylases: versatile regulators, *Trends Genet.* 19 (2003) 286-293.
- [8] M. Haberland, R.L. Montgomery, E.N. Olson, The many roles of histone deacetylases in development and physiology: implications for disease and therapy, *Nat. Rev. Genet.* 10 (2009) 32-42.
- [9] A.J. de Ruijter, A.H. van Gennip, H.N. Caron, S. Kemp, A.B. van Kuilenburg, Histone deacetylases (HDACs): characterization of the classical HDAC family, *Biochem. J.* 370 (2003) 737-749.
- [10] R.W. Johnstone, Histone-deacetylase inhibitors: novel drugs for the treatment of cancer, *Nat. Rev. Drug Discov.* 1 (2002) 287-299.
- [11] S. Emanuele, M. Lauricella, G. Tesoriere, Histone deacetylase inhibitors: apoptotic effects and clinical implications (Review), *Int. J. Oncol.* 33 (2008) 637-646.
- [12] M. Dokmanovic, C. Clarke, P.A. Marks, Histone deacetylase inhibitors: overview and perspectives, *Mol. Cancer Res.* 5 (2007) 981-989.
- [13] I.V. Gregoret, Y.M. Lee, H.V. Goodson, Molecular evolution of the histone deacetylase family: functional implications of phylogenetic analysis, *J. Mol. Biol.* 338 (2004) 17-31.

- [14] J.H. Kalin, J.A. Bergman, Development and therapeutic implications of selective histone deacetylase 6 inhibitors, *J. Med. Chem.* 56 (2013) 6297-6313.
- [15] M. Paris, M. Porcelloni, M. Binaschi, D. Fattori, Histone deacetylase inhibitors: from bench to clinic, *J. Med. Chem.* 51 (2008) 1505-1529.
- [16] C.H. Arrowsmith, C. Bountra, P.V. Fish, K. Lee, M. Schapira, Epigenetic protein families: a new frontier for drug discovery, *Nat. Rev. Drug Discovery* 11 (2012) 384-400.
- [17] F. Thaler, C. Mercurio, Towards Selective Inhibition of Histone Deacetylase Isoforms: What Has Been Achieved, Where We Are and What Will Be Next, *ChemMedChem*, 9 (2014) 523-536.
- [18] J.M. Wagner, B. Hackanson, M. Lubbert, M. Jung, Histone deacetylase (HDAC) inhibitors in recent clinical trials for cancer therapy, *Clin. Epigenet.* 1 (2010) 117-136.
- [19] C. Campas-Moya, Romidepsin for the treatment of cutaneous T-cell lymphoma, *Drugs Today* 45 (2009) 787-795.
- [20] H.M. Prince, M. Dickinson, A. Khot, Romidepsin for cutaneous T-cell lymphoma, *Future Oncol.* 9 (2013) 1819-1827.
- [21] P.A. Marks, R. Breslow, Dimethyl sulfoxide to vorinostat: Development of this histone deacetylase inhibitor as an anticancer drug, *Nat. Biotechnol.* 25 (2007) 84-90.
- [22] R.M. Poole, Belinostat: first global approval, *Drugs* 74 (2014) 1543-1554.
- [23] A. Scuto, M. Kirschbaum, C. Kowolik, L. Kretzner, A. Juhasz, P. Atadja, V. Pullarkat, R. Bhatia, S. Forman, Y. Yen, R. Jove, The novel histone deacetylase inhibitor, LBH589, induces expression of DNA damage response genes and apoptosis in Ph- acute lymphoblastic leukemia cells, *Blood* 111 (2008) 5093-5100.
- [24] M.C. Crisanti, A.F. Wallace, V. Kapoor, F. Vandermeers, M.L. Dowling, L.P. Pereira, K. Coleman, B.G. Campling, Z.G. Fridlender, G.D. Kao, S.M. Albelda, The HDAC inhibitor panobinostat (LBH589) inhibits mesothelioma and lung cancer cells in vitro and in vivo with particular efficacy for small cell lung cancer, *Mol. Cancer Ther.* 8 (2009) 2221-2231.
- [25] M. Guha, HDAC inhibitors still need a home run, despite recent approval, *Nat. Rev. Drug Discov.* 14 (2015) 225-226.
- [26] S.S. Ramalingam, C.P. Belani, C. Ruel, P. Frankel, B. Gitlitz, M. Koczywas, I. Espinoza-Delgado, D. Gandara, Phase II study of belinostat (PXD101), a histone deacetylase inhibitor, for

second line therapy of advanced malignant pleural mesothelioma, *J. Thorac. Oncol.* 4 (2009) 97-101.

[27] H.J. Mackay, H. Hirte, T. Colgan, A. Covens, K. MacAlpine, P. Grenci, L. Wang, J. Mason, P.A. Pham, M.S. Tsao, J. Pan, J. Zwiebel, A.M. Oza, Phase II trial of the histone deacetylase inhibitor belinostat in women with platinum resistant epithelial ovarian cancer and micropapillary (LMP) ovarian tumours, *Eur. J. Cancer* 46 (2010) 1573-1579.

[28] T. Reid, F. Valone, W. Lipera, D. Irwin, W. Paroly, R. Natale, S. Sreedharan, H. Keer, B. Lum, F. Scappaticci, A. Bhatnagar, Phase II trial of the histone deacetylase inhibitor pivaloyloxymethyl butyrate (Pivanex, AN-9) in advanced non-small cell lung cancer, *Lung Cancer* 45 (2004) 381-386.

[29] Y. Bumber, A. Younes, G. Garcia-Manero, Mocetinostat (MGCD0103): a review of an isotype-specific histone deacetylase inhibitor, *Expert Opin. Invest. Drugs* 20 (2011) 823-829.

[30] J. Fraczek, T. Vanhaecke, V. Rogiers, Toxicological and metabolic considerations for histone deacetylase inhibitors, *Expert Opin. Drug Metab. Toxicol.* 9 (2013) 441-457.

[31] L. Loudni, J. Roche, V. Potiron, J. Clarhaut, C. Bachmann, J.P. Gesson, I. Tranoy-Opalinski, Design, synthesis and biological evaluation of 1,4-benzodiazepine-2,5-dione-based HDAC inhibitors, *Bioorg. Med. Chem. Lett.* 17 (2007) 4819-4823.

[32] L. Guandalini, C. Cellai, A. Laurenzana, S. Scapecchi, F. Paoletti, M.N. Romanelli, Design, synthesis and preliminary biological evaluation of new hydroxamate histone deacetylase inhibitors as potential antileukemic agents, *Bioorg. Med. Chem. Lett.* 18 (2008) 5071-5074.

[33] L. Guandalini, M. Balliu, C. Cellai, M.V. Martino, A. Nebbioso, C. Mercurio, V. Carafa, G. Bartolucci, S. Dei, D. Manetti, E. Teodori, S. Scapecchi, L. Altucci, F. Paoletti, M.N. Romanelli, Design, synthesis and preliminary evaluation of a series of histone deacetylase inhibitors carrying a benzodiazepine ring, *Eur. J. Med. Chem.* 66 (2013) 56-68.

[34] M. Balliu, L. Guandalini, M.N. Romanelli, M. D'Amico, F. Paoletti, HDAC-inhibitor (S)-8 disrupts HDAC6-PP1 complex prompting A375 melanoma cell growth arrest and apoptosis, *J. Cell. Mol. Med.* 19 (2015) 143-154.

[35] D.N. Reddy, F. Ballante, T. Chuang, A. Pirolli, B. Marrocco, G.R. Marshall, Design and Synthesis of Simplified Largazole Analogues as Isoform-Selective Human Lysine Deacetylase Inhibitors, *J. Med. Chem.* 59 (2016) 1613-1633.

- [36] A. Saito, T. Yamashita, Y. Mariko, Y. Nosaka, K. Tsuchiya, T. Ando, T. Suzuki, T. Tsuruo, O. Nakanishi, A synthetic inhibitor of histone deacetylase, MS-27-275, with marked in vivo antitumor activity against human tumors, *Proc. Natl. Acad. Sci. U.S.A.* 96 (1999) 4592-4597.
- [37] A. Bowers, N. West, J. Taunton, S.L. Schreiber, J.E. Bradner, R.M. Williams, Total synthesis and biological mode of action of largazole: a potent class I histone deacetylase inhibitor, *J. Am. Chem. Soc.* 130 (2008) 11219-11222.
- [38] S. Balasubramanian, J. Ramos, W. Luo, M. Sirisawad, E. Verner, J.J. Buggy, A novel histone deacetylase 8 (HDAC8)-specific inhibitor PCI-34051 induces apoptosis in T-cell lymphomas, *Leukemia* 22 (2008) 1026-1034.
- [39] Q. Wang, B.A. Rosa, B. Nare, K. Powell, S. Valente, D. Rotili, A. Mai, G.R. Marshall, M. Mitreva, Targeting Lysine Deacetylases (KDACs) in Parasites, *PLoS Negl. Trop. Dis.* 9 (2015) e0004026.
- [40] D.M. Vigushin, S. Ali, P.E. Pace, N. Mirsaidi, K. Ito, I. Adcock, R.C. Coombes, Trichostatin A is a histone deacetylase inhibitor with potent antitumor activity against breast cancer in vivo, *Clin. Cancer Res.* 7 (2001) 971-976.
- [41] K.V. Butler, J. Kalin, C. Brochier, G. Vistoli, B. Langley, A.P. Kozikowski, Rational design and simple chemistry yield a superior, neuroprotective HDAC6 inhibitor, tubastatin A, *J. Am. Chem. Soc.* 132 (2010) 10842-10846.
- [42] T. Suzuki, Y. Kasuya, Y. Itoh, Y. Ota, P. Zhan, K. Asamitsu, H. Nakagawa, T. Okamoto, N. Miyata, Identification of highly selective and potent histone deacetylase 3 inhibitors using click chemistry-based combinatorial fragment assembly, *PLoS One* 8 (2013) e68669.
- [43] V.M. Richon, Y. Webb, R. Merger, T. Sheppard, B. Jursic, L. Ngo, F. Civoli, R. Breslow, R.A. Rifkind, P.A. Marks, Second generation hybrid polar compounds are potent inducers of transformed cell differentiation, *Proc. Natl. Acad. Sci. U.S.A.* 93 (1996) 5705-5708.
- [44] L. Whitehead, M.R. Dobler, B. Radetich, Y. Zhu, P.W. Atadja, T. Claiborne, J.E. Grob, A. McRiner, M.R. Pancost, A. Patnaik, W. Shao, M. Shultz, R. Tichkule, R.A. Tommasi, B. Vash, P. Wang, T. Stams, Human HDAC isoform selectivity achieved via exploitation of the acetate release channel with structurally unique small molecule inhibitors, *Bioorg. Med. Chem.* 19 (2011) 4626-4634.
- [45] F. Ballante, G.R. Marshall, An Automated Strategy for Binding-Pose Selection and Docking Assessment in Structure-Based Drug Design, *J. Chem. Inf. Model.* 56 (2016) 54-72.

- [46] Y. Hai, D.W. Christianson, Histone deacetylase 6 structure and molecular basis of catalysis and inhibition, *Nature chemical biology*, 12 (2016) 741-747.
- [47] Y. Miyake, J.J. Keusch, L.L. Wang, M. Saito, D. Hess, X.N. Wang, B.J. Melancon, P. Helquist, H. Gut, P. Matthias, Structural insights into HDAC6 tubulin deacetylation and its selective inhibition, *Nat. Chem. Biol.* 12 (2016) 748-754.
- [48] A. Vannini, C. Volpari, G. Filocamo, E.C. Casavola, M. Brunetti, D. Renzoni, P. Chakravarty, C. Paolini, R. De Francesco, P. Gallinari, C. Steinkuhler, S. Di Marco, Crystal structure of a eukaryotic zinc-dependent histone deacetylase, human HDAC8, complexed with a hydroxamic acid inhibitor, *Proc. Natl. Acad. Sci. U.S.A.* 101 (2004) 15064-15069.
- [49] A.N. Jain, Surflex-Dock 2.1: robust performance from ligand energetic modeling, ring flexibility, and knowledge-based search, *J. Comput.-Aided Mol. Des.* 21 (2007) 281-306.
- [50] R.A. Laskowski, M.B. Swindells, LigPlot+: multiple ligand-protein interaction diagrams for drug discovery, *J. Chem. Inf. Model.* 51 (2011) 2778-2786.
- [51] GraphPad, in, La Jolla California USA (2012).
- [52] Y. Ying, K. Taori, H. Kim, J. Hong, H. Luesch, Total synthesis and molecular target of largazole, a histone deacetylase inhibitor, *J. Am. Chem. Soc.* 130 (2008) 8455-8459.
- [53] H.M. Berman, J. Westbrook, Z. Feng, G. Gilliland, T.N. Bhat, H. Weissig, I.N. Shindyalov, P.E. Bourne, The Protein Data Bank, *Nucleic Acids Res.* 28 (2000) 235-242.
- [54] B. Webb, A. Sali, Comparative Protein Structure Modeling Using MODELLER, *Curr. Protoc Bioinformatics* 47 (2014), 5.6.1-5.6.32.
- [55] D. Van Der Spoel, E. Lindahl, B. Hess, G. Groenhof, A.E. Mark, H.J. Berendsen, GROMACS: fast, flexible, and free, *J. Comput. Chem.* 26 (2005) 1701-1718.
- [56] K. Lindorff-Larsen, S. Piana, K. Palmo, P. Maragakis, J.L. Klepeis, R.O. Dror, D.E. Shaw, Improved side-chain torsion potentials for the Amber ff99SB protein force field, *Proteins* 78 (2010) 1950-1958.
- [57] W.L. Jorgensen, J. Chandrasekhar, J.D. Madura, R.W. Impey, M.L. Klein, Comparison of Simple Potential Functions for Simulating Liquid Water, *J. Chem. Phys.* 79 (1983) 926-935.
- [58] N.M. O'Boyle, M. Banck, C.A. James, C. Morley, T. Vandermeersch, G.R. Hutchison, Open Babel: An open chemical toolbox, *J. Cheminf.* 3 (2011) 33.

Highlights

- 108 benzodiazepine (BZD) derivatives have been designed and synthesized.
- 104 BZDs were biochemically tested against hKDAC1, 3, 6 and 8 and found active.
- Compound **6q** shows an interesting selectivity against hKDAC3.
- Molecular docking studies have been extensively performed.
- Structure-activity relationships have been rationalized in a pharmacophore scheme.